Waves Random Media **12** (2002) R25–R52 PII: S0959-7174(02)36967-2

TOPICAL REVIEW

Nonlinear photonic crystals: II. Interaction classification for quadratic nonlinearities

Anatoli Babin and Alexander Figotin

Department of Mathematics, University of California at Irvine, CA 92697, USA

Received 10 May 2002, in final form 25 July 2002
Published 11 September 2002
Online at stacks.iop.org/WRM/12/R25

Abstract

Weakly nonlinear interactions between wavepackets in lossless periodic dielectric media are studied based on the classical nonlinear Maxwell equations. We consider nonlinear processes such that: (i) the amplitude of the wave component due to the nonlinearity does not exceed the amplitude of its linear component; (ii) the spatial range of a probing wavepacket is much smaller than the dimension of the medium sample, and it is not too small compared with the dimension of the primitive cell. These nonlinear processes are naturally described in terms of the Bloch modes and the dispersion relations of the underlying linear periodic medium. It turns out that only a few triads of modes have significant nonlinear interactions. They are singled out by the frequency and phase matching conditions and, as we show, by an additional selection rule: the group velocity matching condition. The latter condition is the most important selection rule for the nonlinear regimes. We give a complete quantitative classification of all possible significant interactions for quadratic nonlinearities. The classification is based on a universal system of indices reflecting the intensity of nonlinear interactions. The obtained classification points to the second harmonic generation as being one of the stronger nonlinear interactions, and often the strongest one.

(Some figures in this article are in colour only in the electronic version)

1. Introduction

The effect of the spatial periodicity on nonlinear optical processes, especially of media with a quadratic nonlinearity, has been the subject of intensive studies in physical literature [1–4, 8–10, 13–15, 20–24, 30, 33, 34, 36, 37, 40–42, 44, 45, 48–50, 52, 53, 58, 63, 65] and references therein. In this paper we essentially finalize the classification of weakly nonlinear interactions for quadratic nonlinearities within the framework developed in the preceding paper [12]. In particular, we introduce a natural extension of the group velocity concept to singular points where the standard group velocity does not apply. This allows us to single out the group velocity matching condition (GVC) as a universal and most important selection rule for significant weakly nonlinear interactions.

We study weakly nonlinear phenomena satisfying the following basic conditions: (i) the amplitude of the wave component due to the nonlinearity does not exceed the amplitude of its linear component and (ii) the wavepacket spatial range is much smaller than the dimension of the medium sample, and it is not too small compared with the dimension of the primitive cell. These phenomena can be naturally studied based on the underlying linear medium as a reference frame. We would like to point out that weakly nonlinear phenomena *do not require small nonlinear susceptibilities* which can be whatever they happen to be. The term 'weak' rather refers to appropriately small initial amplitudes of the electromagnetic (EM) wave. Under this condition, and in the presence of nonlinearities the linear wave evolution undergoes incremental changes until the nonlinear effects accumulate to a level comparable to the level of the relevant linear wave.

It is assumed that the electromagnetic wave propagation is described by the classical Maxwell equations

$$\nabla \times \boldsymbol{E}(\boldsymbol{r}, t) = -\frac{1}{c}\partial_t \boldsymbol{B}(\boldsymbol{r}, t) - \frac{4\pi}{c}\boldsymbol{J}_M(\boldsymbol{r}, t), \qquad \nabla \cdot \boldsymbol{B}(\boldsymbol{r}, t) = 0, \tag{1}$$

$$\nabla \times \boldsymbol{H}(\boldsymbol{r}, t) = \frac{1}{c}\partial_t \boldsymbol{D}(\boldsymbol{r}, t) + \frac{4\pi}{c}\boldsymbol{J}_E(\boldsymbol{r}, t), \qquad \nabla \cdot \boldsymbol{D}(\boldsymbol{r}, t) = 0, \tag{2}$$

where $\boldsymbol{H}$, $\boldsymbol{E}$, $\boldsymbol{B}$ and $\boldsymbol{D}$ are respectively the magnetic and electric fields, magnetic and electric inductions, and $\boldsymbol{J}_E$ and $\boldsymbol{J}_M$ are the excitation electric and, so-called, excitation magnetic currents (current sources). It is also assumed that *there are no free electric and magnetic charges*, and, consequently, the fields $\boldsymbol{B}$ and $\boldsymbol{D}$ are divergence free as indicated in equations (1) and (2). Equations (1) and (2) readily imply that the excitation electric and magnetic currents are also divergence free, i.e.

$$\nabla \cdot \boldsymbol{J}_E(\boldsymbol{r}, t) = 0, \qquad \nabla \cdot \boldsymbol{J}_M(\boldsymbol{r}, t) = 0. \tag{3}$$

We use the excitation currents primarily to generate wavepackets playing the key role in the analysis of nonlinear phenomena. For simplicity we consider nonmagnetic media, i.e.

$$\boldsymbol{B}(\boldsymbol{r}, t) = \mu \boldsymbol{H}(\boldsymbol{r}, t), \qquad \mu = 1. \tag{4}$$

The material relations between $\boldsymbol{D}$ and $\boldsymbol{E}$ are assumed to be of the standard form [16]

$$\boldsymbol{D} = \boldsymbol{E} + 4\pi \boldsymbol{P}(\boldsymbol{r}, t; \boldsymbol{E}) \tag{5}$$

where the polarization $\boldsymbol{P}$ includes both the linear and the nonlinear parts

$$\boldsymbol{P}(\boldsymbol{r}, t; \boldsymbol{E}(\cdot)) = \boldsymbol{P}^{(1)}(\boldsymbol{r}, t; \boldsymbol{E}(\cdot)) + \boldsymbol{P}_{\mathrm{NL}}(\boldsymbol{r}, t; \boldsymbol{E}(\cdot)). \tag{6}$$

The nonlinear part $\boldsymbol{P}_{\mathrm{NL}}(\boldsymbol{r}, t; \boldsymbol{E}(\cdot))$ is often assumed to be homogeneous in $\boldsymbol{E}(\cdot)$ of the order $h \geqslant 2$, $h = 2$ for a quadratic and $h = 3$ for a cubic nonlinearity [16, 17]. To quantify the relative impact of the nonlinearity we introduce a dimensionless constant α_0 and scale all the fields as follows:

$$\begin{aligned} &\boldsymbol{J}_E \to \alpha_0 \boldsymbol{J}_E, \qquad \boldsymbol{J}_M \to \alpha_0 \boldsymbol{J}_M, \qquad \boldsymbol{E} \to \alpha_0 \boldsymbol{E}, \\ &\boldsymbol{D} \to \alpha_0 \boldsymbol{D}, \qquad \boldsymbol{H} \to \alpha_0 \boldsymbol{H}, \qquad \boldsymbol{B} \to \alpha_0 \boldsymbol{B}. \end{aligned} \tag{7}$$

Then the magnitude of the rescaled nonlinearity $\tilde{\boldsymbol{P}}_{\mathrm{NL}}(\tilde{\boldsymbol{E}})$ is of order $\alpha = \alpha_0^{h-1}$ for $\alpha_0 \ll 1$, and the material relation becomes

$$\boldsymbol{D} = \boldsymbol{E} + 4\pi[\boldsymbol{P}^{(1)}(\boldsymbol{r}, t; \boldsymbol{E}(\cdot)) + \alpha \boldsymbol{P}_{\mathrm{NL}}(\boldsymbol{r}, t; \boldsymbol{E}; \alpha)], \qquad \alpha = \alpha_0^{h-1} \ll 1 \tag{8}$$

where $\alpha \ll 1$ measures the relative magnitude of the nonlinearity. We allow for $\boldsymbol{P}_{\mathrm{NL}}$ a general analytic dependence in $\boldsymbol{E}$ with $h_0 \geqslant 2$ being the order of the leading term, namely

$$\boldsymbol{P}_{\mathrm{NL}}(\boldsymbol{r}, t; \boldsymbol{E}) = \boldsymbol{P}^{(h_0)}(\boldsymbol{r}, t; \boldsymbol{E}) + \sum_{h>h_0}^{\infty} \boldsymbol{P}^{(h)}(\boldsymbol{r}, t; \boldsymbol{E}; \alpha) \tag{9}$$

where $\boldsymbol{P}^{(h)}(\boldsymbol{E})$ are h-linear (tensorial) operators. In view of (8), the leading term $\boldsymbol{P}^{(h_0)}(\boldsymbol{E})$ does not depend on α. According to the classical nonlinear optics, see [16] (section 2), $\boldsymbol{P}^{(h)}$ has the following form:

$$\boldsymbol{P}^{(h)}(\boldsymbol{r}, t; \boldsymbol{E}(\cdot); \alpha) = \int_{-\infty}^{t} \dots \int_{-\infty}^{t} P^{(h)}(\boldsymbol{r}; t - t_1, \dots, t - t_h; \alpha) \vdots \prod_{j=1}^{h} \boldsymbol{E}(\boldsymbol{r}, t_j)\, \mathrm{d}t_j, \tag{10}$$

where $P^{(h)}$ is the so-called h-order polarization response function. For fixed $\boldsymbol{r}$ and $t - t_j$ the quantity $\boldsymbol{P}^{(h)}$ is an h-linear tensor acting on the components of $\boldsymbol{E}(\boldsymbol{r}, t_j)$. This form of the polarization response function in (10) takes explicitly into account *two fundamental properties of the medium: the time-invariance and the causality* [16] (section 2).

The linear part $\boldsymbol{P}^{(1)}(\boldsymbol{r}, t; \boldsymbol{E}(\cdot))$ of the total polarization is given by

$$\boldsymbol{P}^{(1)}(\boldsymbol{r}, t; \boldsymbol{E}(\cdot)) = \boldsymbol{\chi}^{(1)}(\boldsymbol{r})\boldsymbol{E}(\boldsymbol{r}, t) \tag{11}$$

where $\boldsymbol{\chi}^{(1)}(\boldsymbol{r})$ is the tensor of linear susceptibility. For simplicity of rigorous argumentation we assume that $\boldsymbol{\chi}^{(1)}(\boldsymbol{r})$ does not depend on the frequency that, from physical point of view, efficiently binds us to a certain frequency range. We would like to emphasize that this simplifying assumption does not affect the analysis of nonlinear interactions since it takes as a 'starting point' the dispersion relations of the linear medium, whatever they happen to be [12].

It is preferable to deal with divergence-free fields [12], and for that reason we choose $\boldsymbol{D}$ to be our basic field. To implement this, we recast (8) as

$$\boldsymbol{E}(\boldsymbol{r}, t) = \boldsymbol{\eta}^{(1)}(\boldsymbol{r})\boldsymbol{D}(\boldsymbol{r}, t) - \alpha \boldsymbol{S}(\boldsymbol{r}, t; \boldsymbol{D}; \alpha), \tag{12}$$

$$\boldsymbol{\eta}^{(1)}(\boldsymbol{r}) = [\varepsilon^{(1)}(\boldsymbol{r})]^{-1}, \qquad \varepsilon^{(1)}(\boldsymbol{r}) = 1 + 4\pi\boldsymbol{\chi}^{(1)}(\boldsymbol{r}), \tag{13}$$

where $\varepsilon^{(1)}(\boldsymbol{r})$ and $\boldsymbol{\eta}^{(1)}(\boldsymbol{r})$ are respectively tensors of the dielectric permittivity and the impermeability. The latter is commonly used in the studies of the electro-optical effects (Pockels and Kerr effects) [62] (section 7), [47] (sections 6.3, 18.1).

The dielectric properties of the periodic medium are assumed to vary periodically in space. In other words, the tensors $\boldsymbol{\chi}^{(1)}(\boldsymbol{r})$, $\boldsymbol{\eta}^{(1)}(\boldsymbol{r})$ and $\boldsymbol{P}_{\mathrm{NL}}(\boldsymbol{r}, t; \boldsymbol{E}; \alpha)$, $\boldsymbol{S}(\boldsymbol{r}, t; \boldsymbol{D}; \alpha)$ are periodic functions of the position $\boldsymbol{r}$. In particular, if the lattice of periods is cubic with the lattice constant L_0, and $\mathbb{Z}^3$ is the lattice of integer valued vectors $\boldsymbol{n}$, then the following periodicity conditions hold for every $\boldsymbol{n}$ from $\boldsymbol{Z}^3$:

$$\boldsymbol{\eta}^{(1)}(\boldsymbol{r} + L_0\boldsymbol{n}) = \boldsymbol{\eta}^{(1)}(\boldsymbol{r}), \qquad P^{(h)}(\boldsymbol{r} + L_0\boldsymbol{n}; t_1, \dots, t_h; \alpha) = P^{(h)}(\boldsymbol{r}; t_1, \dots, t_h; \alpha). \tag{14}$$

Substituting $\boldsymbol{E}$ determined by (12) into the Maxwell equations (1), (2), we rewrite them in the following concise form:

$$\partial_t \boldsymbol{U} = -\mathrm{i}\mathcal{M}\boldsymbol{U} + \alpha \boldsymbol{F}_{\mathrm{NL}}(\boldsymbol{U}) - \boldsymbol{J}; \qquad \boldsymbol{U}(t) = 0 \text{ for } t \leqslant 0, \tag{15}$$

where

$$\boldsymbol{U} = \begin{bmatrix} \boldsymbol{D} \\ \boldsymbol{B} \end{bmatrix}, \qquad \mathcal{M}\boldsymbol{U} = \mathrm{i}\begin{bmatrix} \nabla \times \boldsymbol{B} \\ -\nabla \times (\boldsymbol{\eta}^{(1)}(\boldsymbol{r})\boldsymbol{D}) \end{bmatrix}, \tag{16}$$

$$\boldsymbol{J} = 4\pi \begin{bmatrix} \boldsymbol{J}_E \\ \boldsymbol{J}_M \end{bmatrix}, \qquad \boldsymbol{F}_{\mathrm{NL}}(\boldsymbol{U}) = \begin{bmatrix} \boldsymbol{0} \\ \nabla \times \boldsymbol{S}(\boldsymbol{r}, t; \boldsymbol{D}) \end{bmatrix}, \tag{17}$$

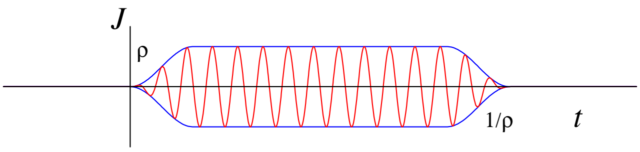

Figure 1. Impressed current J in the form of wavepacket of amplitude of order ϱ and of time length of order $1/\varrho$ causes the medium nonlinear response. Based on this response we estimate the rates of energy exchange between different modes.

assuming everywhere that all the fields $\boldsymbol{D}$, $\boldsymbol{B}$, $\boldsymbol{J}_E$ and $\boldsymbol{J}_M$ are divergence free. We also assume that the medium is at rest for all negative times by requiring the excitation currents $\boldsymbol{J}$ to vanish for all negative times, i.e.

$$\boldsymbol{J}(t) = 0 \qquad \text{for } t \leqslant 0. \tag{18}$$

Observe that in the operator form (15) of the Maxwell equations the parameter α determines the relative magnitude of the nonlinearity, and, in particular, if $\alpha = 0$ the medium evidently becomes linear.

1.1. Outline of the nonlinear interaction classification

In this section we provide a less technical outline of our approach to the classification of nonlinear interactions. For the clarity of the argument we assume the photonic crystal to occupy the entire space. The approach begins with probing the dielectric medium with the excitation current $\boldsymbol{J}$ of sufficiently small amplitude α_0 and of the relative bandwidth $\varrho \sim \Delta\omega/\omega_0$, where $\Delta\omega$ is the frequency bandwidth of the wavepacket and ω_0 is its carrier frequency (see figure 1).

The medium response $\boldsymbol{U}(t)$ to the excitation current $\boldsymbol{J}$ has the form

$$\boldsymbol{U}(t) = \boldsymbol{U}^{(0)}(t) + \alpha \boldsymbol{U}^{(1)}(t) + \mathrm{O}(\alpha^2), \tag{19}$$

where $\boldsymbol{U}^{(0)}(t)$ is the linear medium response and $\boldsymbol{U}^{(1)}(t)$ is the first nonlinear response. The first nonlinear response $\boldsymbol{U}^{(1)}(t)$ becomes appreciable for times $t \gtrsim \varrho^{-1}$.

To classify nonlinear interactions between the modes we study the first nonlinear response $\boldsymbol{U}^{(1)}$ and its behaviour as $\varrho \to 0$. The first step is to decompose all the fields with respect to the Bloch modes of the underlying medium. These modes are parametrized by $(\bar{n}, \boldsymbol{k})$ where $\bar{n}$ is the band number and $\boldsymbol{k}$ is the quasimomentum. It is well known that for a quadratic nonlinearity the energy exchange between the modes occurs through triads of modes $(\bar{n}, \boldsymbol{k})$, $(\bar{n}', \boldsymbol{k}')$ and $(\bar{n}'', \boldsymbol{k}'')$ with the corresponding dispersion relations $\omega_{\bar{n}}(\boldsymbol{k})$, $\omega_{\bar{n}'}(\boldsymbol{k}')$ and $\omega_{\bar{n}''}(\boldsymbol{k}'')$. In view of the phase matching condition, we always have $\boldsymbol{k}'' = \boldsymbol{k} - \boldsymbol{k}'$. To analyse the interactions, we look at the impact of the modes $(\bar{n}', \boldsymbol{k}')$ and $(\bar{n}'', \boldsymbol{k} - \boldsymbol{k}')$ on the mode $(\bar{n}, \boldsymbol{k})$, and see that the amplitude of the first nonlinear response $\tilde{U}_{\bar{n}}^{(1)}(\boldsymbol{k})$ depends on the amplitudes of the linear response $\tilde{U}_{\bar{n}'}^{(0)}(\boldsymbol{k}')$ and $\tilde{U}_{\bar{n}''}^{(0)}(\boldsymbol{k} - \boldsymbol{k}')$. Let us denote the contribution of amplitudes $\tilde{U}_{\bar{n}'}^{(0)}(\boldsymbol{k}')$ and $\tilde{U}_{\bar{n}''}^{(0)}(\boldsymbol{k} - \boldsymbol{k}')$ to the amplitude $\tilde{U}_{\bar{n}}^{(1)}(\boldsymbol{k})$ by $\tilde{U}^{(1)}(\bar{n}, \bar{n}', \bar{n}'', \boldsymbol{k}', \boldsymbol{k})$. It is shown in [12] that if $\varrho \to 0$ the first nonlinear response $\boldsymbol{U}^{(1)}$ vanishes as a power of ϱ, namely

$$\tilde{U}^{(1)}(\bar{n}, \bar{n}', \bar{n}'', \boldsymbol{k}', \boldsymbol{k}) \sim \varrho^q, \qquad \varrho \to 0 \text{ where } 0 < q \leqslant \infty. \tag{20}$$

If, for instance, the modes $(\bar{n}, \boldsymbol{k})$, $(\bar{n}', \boldsymbol{k}')$ and $(\bar{n}'', \boldsymbol{k}'')$ are chosen 'at random' then the above index q is infinite and, consequently, the mode interaction is weaker than any power of ϱ as $\varrho \to 0$. But for special choices of triads the corresponding indices q can be finite with more appreciable nonlinear interactions. These stronger interacting modes can be singled out with the help of two selection rules based on the corresponding *phase function*

$$\phi_{\bar{n}}(\boldsymbol{k}, \boldsymbol{k}') = \omega_{\bar{n}}(\boldsymbol{k}) - \omega_{\bar{n}'}(\boldsymbol{k}') - \omega_{\bar{n}''}(\boldsymbol{k} - \boldsymbol{k}'), \tag{21}$$

which explicitly takes into account the so-called *phase matching condition* $\boldsymbol{k}'' = \boldsymbol{k} - \boldsymbol{k}'$. The two selection rules are the *frequency matching condition (FMC)*

$$\phi_{\vec{n}}(\boldsymbol{k}, \boldsymbol{k}') = \omega_{\bar{n}}(\boldsymbol{k}) - \omega_{\bar{n}'}(\boldsymbol{k}') - \omega_{\bar{n}''}(\boldsymbol{k} - \boldsymbol{k}') = 0, \tag{22}$$

and the *GVC*

$$\nabla\omega_{\bar{n}'}(\boldsymbol{k}') = \nabla\omega_{\bar{n}''}(\boldsymbol{k} - \boldsymbol{k}'), \tag{23}$$

with the latter following from the stationary phase requirement $\nabla_{\boldsymbol{k}'}\phi_{\vec{n}}(\boldsymbol{k}, \boldsymbol{k}') = 0$.

The relative significance of the two rules is based on their impact on the indices q. As it is shown in [12], if a triad of modes does not satisfy the GVC (23) then, regardless of whether the FMC (22) is satisfied or not, its index $q = \infty$, and, hence, the mode interaction is weaker than any power of ϱ. In contrast, if GVC (23) is satisfied then, regardless of whether the FMC (22) is satisfied or not, the index q can be finite. The FMC (22) though can improve the index by 1 if it is met. In particular, if we seek the strongest nonlinear interaction and the two conditions GVC and FMC cannot be met simultaneously, then GVC is more important to comply with. All possible values for the indices of interaction together with the corresponding canonical polynomial forms for the phase function are collected in the tables presented in section 7.

For the reader's convenience we give a brief account of basic elements of the framework from [12]. The rigorous theoretical analysis is carried out under the asymptotic assumptions

$$\varrho \ll 1, \qquad \alpha \ll 1, \qquad \alpha/\varrho < 1, \tag{24}$$

which allow one to distinguish, classify and study a number of nonlinear wave interactions in photonic crystals including, in particular, second harmonic generation (SHG). The construction of wavepackets probing the medium together with the consequent analysis of related nonlinear effects is based on the spectral theory of the underlying linear periodic medium. Proper wavepackets are produced by the currents $\boldsymbol{J}(t)$ of the form of a slowly modulated carrier wave (see figure 1)

$$\boldsymbol{J}(t) = \varrho \mathrm{e}^{-\mathrm{i}\mathcal{M}t}\boldsymbol{j}(\tau) = \varrho \mathrm{e}^{-\mathrm{i}\frac{\mathcal{M}}{\varrho}\tau}\boldsymbol{j}(\tau), \qquad \tau = \varrho t \tag{25}$$

$$\text{where } j(\tau) = 0 \qquad \text{for } \tau \leqslant 0. \tag{26}$$

This introduces into consideration a new *slow time* scale τ. Note that the term $\mathrm{e}^{-\mathrm{i}\mathcal{M}t}\boldsymbol{j}$ in (25) with constant $\boldsymbol{j}$ solves the linear problem $\partial_t \boldsymbol{u} = -\mathrm{i}\mathcal{M}\boldsymbol{u}$, $\boldsymbol{u}(0) = \boldsymbol{j}$. This solution can be written explicitly in terms of the Floquet–Bloch eigenmodes. The *slow time* $\tau = \varrho t$ is a natural scale for the time evolution of the nonlinear processes under study. Note also that the condition (26) implies that for negative times everything is at rest and

$$\boldsymbol{U}(t) = 0, \qquad t \leqslant 0. \tag{27}$$

If a current of the form (25), (26) is introduced in the linear medium, it produces a wavepacket $\boldsymbol{U}^{(0)}$ described by

$$\boldsymbol{U}^{(0)} = \mathrm{e}^{-\mathrm{i}\mathcal{M}t}\boldsymbol{V}^{(0)}(\tau), \qquad \boldsymbol{V}^{(0)}(\tau) = -\int_0^\tau \boldsymbol{j}(\tau_1)\,\mathrm{d}\tau_1, \tag{28}$$

where, in view of (26), $\boldsymbol{V}^{(0)}(\tau) = 0$ if $\tau \leqslant 0$. To single out the first nonlinear response we represent $\boldsymbol{U}(t)$ as

$$\boldsymbol{U}(t) = \mathrm{e}^{-\mathrm{i}\mathcal{M}t}\boldsymbol{V}(\tau), \qquad \boldsymbol{V}(\tau) = \boldsymbol{W}(\tau) + \boldsymbol{V}^{(0)}(\tau), \tag{29}$$

where $\boldsymbol{V}^{(0)}$ is defined by (28). Clearly $\boldsymbol{V}(\tau)$ and $\boldsymbol{W}(\tau)$ vanish for negative times. Then, as it is shown in [12], the first nonlinear response is given by

$$\boldsymbol{U}^{(1)}(t) = \mathrm{e}^{-\mathrm{i}\mathcal{M}t}\boldsymbol{V}^{(1)}(\tau), \qquad \boldsymbol{V}^{(1)}(\tau) = \frac{\alpha}{\varrho}\int_0^\tau \mathrm{e}^{\mathrm{i}\frac{\mathcal{M}}{\varrho}\tau_1}\boldsymbol{F}_{\mathrm{NL}}[\mathrm{e}^{-\mathrm{i}\frac{\mathcal{M}}{\varrho}\tau_1}\boldsymbol{V}^{(0)}(\tau_1)]\,\mathrm{d}\tau_1. \tag{30}$$

The representation of the first nonlinear response $\boldsymbol{V}^{(1)}(\tau)$ by the oscillatory integral in (30) plays the central role in the studies of nonlinear wave interactions in photonic crystals.

The studies are carried out for one-, two- and three-dimensional dielectric media with a quadratic nonlinearity. Most of the analysis below is presented for the more difficult case of the three-dimensional space.

1.2. Range of applicability

The nonlinear phenomena in photonic crystals which we study have limitations due to the choices of probing waves. Our probing waves are combinations of a number of almost monochromatic elementary wavepackets. Every elementary wavepacket has its carrier frequency which, for instance, can be thought of as belonging to one channel in a multichannel system.

The limitations on probing elementary wavepackets stem primarily from the condition of their almost monochromaticity $\varrho = \frac{\Delta\omega}{\omega_0} \ll 1$, and the natural condition that the wavepacket must reside in the body of the nonlinear photonic crystal for the time of nonlinear interactions. Note that the inequality $\varrho \ll 1$ implies that the wavepacket has the number of cycles $N_{\mathrm{wp}} = \varrho^{-1} \gg 1$.

The limitations on the intensity of nonlinear interactions stem from the requirement to have the underlying linear medium as an adequate reference frame for the analysis of nonlinear interactions.

The mentioned limitations can be formulated in different ways. The nonlinear regimes under study are best described in terms of the Floquet–Bloch components of the excitation currents and the waves they generate. The conditions describing these regimes can also be formulated rather adequately in simpler terms of the amplitudes and space dimensions of the excitation currents and generated waves. They are as follows.

(i) The spatial range L_{wp} of the excitation currents as well as generated wavepackets is not too small compared with the space dimension L_0 of the primitive cell. This constraint is due to the fact that the probing wavepacket is composed essentially of Bloch eigenmodes from just a few spectral bands. Consequently, due the nature of the Bloch eigenmodes, the wavepacket spatial dimension cannot be much smaller than L_0.

(ii) The space dimension L_{phcryst} of a sample of the nonlinear photonic crystal (nonlinear periodic medium) is much larger than the lattice constant, that is the size of the primitive cell, L_0, i.e. $L_{\mathrm{phcryst}} \gg L_0$.

(iii) The spatial range L_{wp} of wavepackets is much smaller than L_{phcryst}, i.e.

$$L_{\mathrm{wp}} \ll L_{\mathrm{phcryst}}. \tag{31}$$

The condition (31) assures that the wavepacket will stay in the body of the photonic crystal for the time of nonlinear interactions. In fact, for simplicity we study rigorously an ideal situation of an infinitely large photonic crystal $L_{\mathrm{phcryst}} = \infty$.

(iv) The excitation currents are almost harmonic and have sufficiently small amplitudes. We consider the wave time evolution only up to the point where the amplitude of the first nonlinear response does not exceed the amplitude of the wave linear component. Consequently, the underlying linear medium, particularly its dispersion relations, provide a good reference frame for the constructive analysis of the nonlinear regimes under study.

The relation between the inequality $L_{\mathrm{wp}} \ll L_{\mathrm{phcryst}}$ and limitations of the stationary phase method based on the smoothness (differentiability) of the Floquet–Bloch transform of the wave in the quasimomentum $\boldsymbol{k}$ are discussed in section 3.1.

To make a rough order of magnitude assessment of the parameters of an elementary (almost monochromatic) wavepacket with $\frac{\Delta\omega}{\omega_0} = \varrho$ propagating in the photonic crystal, we assume that

(i) it has reference (carrier) frequency ω_0 and the frequency spread $\Delta\omega$;
(ii) its reference wavelength is $\lambda_0 = \omega_0/c$ with c being the speed of light in the crystal;
(iii) k_0 is the reference quasimomentum (wavenumber).

Then in the case when the group velocity $\omega_n'(k_0)$ does not vanish we get the following approximate estimations:

$$\Delta\omega \approx \omega_n'(k_0)\Delta k, \qquad L_{\mathrm{wp}} \approx \frac{2\pi}{\Delta k} \approx \frac{2\pi\omega_n'(k_0)}{\varrho\omega_0} = \frac{\omega_n'(k_0)}{c}\lambda_0 N_{\mathrm{wp}}, \tag{32}$$

for which the limitation (31) reduces to

$$\frac{\omega_n'(k_0)}{c}\lambda_0 N_{\mathrm{wp}} \ll L_{\mathrm{phcryst}}. \tag{33}$$

Observe that the condition (33) is satisfied for sufficiently small group velocity $\omega_n'(k_0)$. For nonlinear interactions related to the SHG with both the fundamental and the second-harmonic frequencies tuned to photonic band edges [23, 48], the condition (33) can be well satisfied. In these cases, when the group velocity $\omega_n'(k_0)$ almost vanishes, assuming that $\omega_n''(k_0)$ does not vanish, we can get a more accurate assessment of the parameters substituting (32) with the following approximation:

$$\Delta\omega \approx \frac{\omega_n''(k_0)}{2}\Delta k^2, \qquad L_{\mathrm{wp}} \approx \frac{2\pi}{\Delta k} \approx \sqrt{\frac{\pi\omega_n''(k_0)}{c}\lambda_0 N_{\mathrm{wp}}}, \tag{34}$$

for which the limitation (31) reduces to

$$\sqrt{\frac{\pi\omega_n''(k_0)}{c}\lambda_0 N_{\mathrm{wp}}} \ll L_{\mathrm{phcryst}}. \tag{35}$$

2. Modal expansions and two time scales

An important step in the studies of nonlinear wave interactions is recasting the evolution equation in the modal form based on the eigenmodes of the underlying linear medium. In fact, the choice of eigenmodes as a basis for waves is absolutely necessary in the analysis of nonlinear phenomena of interest. The special role of the basis of eigenmodes rests on their unique property not to exchange the energy in the course of linear evolution. Any other choice for the basis of the linear medium would result in the mode energy exchange obscuring the nonlinear processes under study [12]. A number of different aspects of nonlinear regimes were studied based on coupled modes approach, Floquet–Bloch spectral decomposition and multiple scales [8, 9, 22, 37, 52].

Thus, let us introduce the eigenmodes of the underlying linear medium as described by the linear Maxwell operator $\mathcal{M}$ in (16). For simplicity, we consider the case when the lattice of periods is cubic with the lattice constant L_0. In addition, we switch to the dimensionless space variable $\boldsymbol{r} \to \boldsymbol{r}L_0^{-1}$, keeping the same notation $\boldsymbol{r}$ for it. Note then that the spatial period becomes 1. Since the coefficients of the differential operator $\mathcal{M}$ are periodic its basic spectral properties are covered by Floquet–Bloch theory [11, 54].

Namely, all the eigenvalues and the eigenmodes of $\mathcal{M}$ are parametrized by two indices: the zone (band) number $n = 1, 2, \ldots,$ and the quasimomentum $\boldsymbol{k}$ from the so-called *Brillouin zone*. In view of (14), the Brillouin zone in our case is the cube $[-\pi, \pi]^3$. Note that the operator

$\mathcal{M}$ has a property that if ω is an eigenfrequency then $-\omega$ is also an eigenfrequency. By Floquet–Bloch theory the spectrum of the periodic operator $\mathcal{M}$ is described by eigenfrequencies

$$\pm\omega_n(\boldsymbol{k}), \qquad n = 1, 2, \ldots, \ \boldsymbol{k} \text{ in } [-\pi, \pi]^3. \tag{36}$$

We assume that the eigenvalues are naturally ordered

$$0 \leqslant \omega_1(\boldsymbol{k}) \leqslant \omega_2(\boldsymbol{k}) \leqslant \cdots. \tag{37}$$

To take into account the negative eigenfrequency we introduce pairs

$$\bar{n} = (\zeta, n) \qquad \text{where } \zeta = \pm 1, \ n = 1, 2, \ldots \tag{38}$$

and set

$$\omega_{\bar{n}}(\boldsymbol{k}) = \zeta\omega_n(\boldsymbol{k}), \qquad \text{for } \bar{n} = (\zeta, n). \tag{39}$$

We remind that the corresponding Bloch eigenmodes $\tilde{\boldsymbol{G}}_{\bar{n}}(\boldsymbol{r}, \boldsymbol{k})$ satisfy the following relations:

$$\mathcal{M}\tilde{\boldsymbol{G}}_{\bar{n}}(\boldsymbol{r}, \boldsymbol{k}) = \omega_{\bar{n}}(\boldsymbol{k})\tilde{\boldsymbol{G}}_{\bar{n}}(\boldsymbol{r}, \boldsymbol{k}), \tag{40}$$

$$\tilde{\boldsymbol{G}}_{\bar{n}}(\boldsymbol{r} + \boldsymbol{m}, \boldsymbol{k}) = \mathrm{e}^{\mathrm{i}\boldsymbol{k}\cdot\boldsymbol{m}}\tilde{\boldsymbol{G}}_{\bar{n}}(\boldsymbol{r}, \boldsymbol{k}), \qquad \boldsymbol{m} \text{ in } \mathbb{Z}^3. \tag{41}$$

In addition to that (see [12] for details),

$$\tilde{\boldsymbol{G}}_{\bar{n}}(\boldsymbol{r}, \boldsymbol{k}) = \begin{bmatrix} \tilde{\boldsymbol{D}}_{\bar{n}}(\boldsymbol{r}, \boldsymbol{k}) \\ \tilde{\boldsymbol{B}}_{\bar{n}}(\boldsymbol{r}, \boldsymbol{k}) \end{bmatrix} = \begin{bmatrix} \mathrm{i}\zeta[\omega_n(\boldsymbol{k})\mu]^{-1}\nabla \times \tilde{\boldsymbol{B}}_{\bar{n}}(\boldsymbol{r}, \boldsymbol{k}) \\ \tilde{\boldsymbol{B}}_{\bar{n}}(\boldsymbol{r}, \boldsymbol{k}) \end{bmatrix}, \tag{42}$$

$$\nabla \cdot \tilde{\boldsymbol{B}}_{\bar{n}}(\boldsymbol{r}, \boldsymbol{k}) = 0, \qquad \nabla \cdot \tilde{\boldsymbol{D}}_{\bar{n}}(\boldsymbol{r}, \boldsymbol{k}) = 0, \tag{43}$$

and the fields $\tilde{\boldsymbol{B}}_{\bar{n}}(\boldsymbol{r}, \boldsymbol{k})$ are of the Bloch form

$$\tilde{\boldsymbol{B}}_{\bar{n}}(\boldsymbol{r}, \boldsymbol{k}) = \mathrm{e}^{\{\mathrm{i}\boldsymbol{k}\cdot\boldsymbol{r}\}}\hat{\boldsymbol{B}}_{\bar{n}}(\boldsymbol{r}, \boldsymbol{k}),$$

where $\hat{\boldsymbol{B}}_{\bar{n}}$ is a $\mathbb{Z}^3$-periodic function in $\boldsymbol{r}$. For every fixed quasimomentum $\boldsymbol{k}$ the eigenfunctions $\tilde{\boldsymbol{G}}_{\bar{n}}(\boldsymbol{r}, \boldsymbol{k})$ of different $\bar{n}$ are orthogonal with respect to the following scalar product:

$$(\boldsymbol{U}_1(\boldsymbol{r}), \boldsymbol{U}_2(\boldsymbol{r})) = \int_{[-1,1]^3} \boldsymbol{U}_1^*(\boldsymbol{r}) \begin{bmatrix} \boldsymbol{\eta}^{(1)}(\boldsymbol{r}) & \boldsymbol{0} \\ \boldsymbol{0} & \boldsymbol{1} \end{bmatrix} \boldsymbol{U}_2(\boldsymbol{r}) \, \mathrm{d}\boldsymbol{r} \tag{44}$$

where $\boldsymbol{U}^*$ stands for a vector conjugate to the complex valued vector $\boldsymbol{U}$. Namely

$$(\tilde{\boldsymbol{G}}_{\bar{n}}(\boldsymbol{r}, \boldsymbol{k}), \tilde{\boldsymbol{G}}_{\bar{n}'}(\boldsymbol{r}, \boldsymbol{k})) = \delta_{\bar{n},\bar{n}'} \tag{45}$$

where $\delta_{\bar{n},\bar{n}'}$ is the Kronecker symbol.

Now for any vector field $\boldsymbol{U}(\boldsymbol{r})$ we introduce its modal expansion

$$\boldsymbol{U}(\boldsymbol{r}) = \frac{1}{(2\pi)^3} \sum_{\bar{n}} \int_{[-\pi,\pi]^3} \tilde{U}_{\bar{n}}(\boldsymbol{k})\tilde{\boldsymbol{G}}_{\bar{n}}(\boldsymbol{r}, \boldsymbol{k}) \, \mathrm{d}\boldsymbol{k}. \tag{46}$$

Observe that the general solution to the linear Maxwell equations, $\alpha = 0$, in the absence of currents takes the form

$$\boldsymbol{U}(\boldsymbol{r}, t) = \sum_{\bar{n}} \int_{[-\pi,\pi]^3} \tilde{U}_{\bar{n}}(\boldsymbol{k})\boldsymbol{G}_{\bar{n}}(\boldsymbol{r}, \boldsymbol{k})\mathrm{e}^{-\mathrm{i}\omega_{\bar{n}}(\boldsymbol{k})t} \, \mathrm{d}\boldsymbol{k} \tag{47}$$

where $\tilde{U}_{\bar{n}}(\boldsymbol{k})$ are the Bloch mode coefficients of $\boldsymbol{U}$.

To use the excitation current $\boldsymbol{J}$ as a wavepacket generation instrument we assume that it has the following modal representation:

$$\boldsymbol{J}(\boldsymbol{r}, t) = \sum_{\bar{n}} \frac{1}{(2\pi)^3} \int_{[-\pi,\pi]^3} \varrho\,\tilde{j}_n(\boldsymbol{k}, \tau)\boldsymbol{G}_{\bar{n}}(\boldsymbol{r}, \boldsymbol{k})\mathrm{e}^{-\mathrm{i}\omega_{\bar{n}}(\boldsymbol{k})t} \, \mathrm{d}\boldsymbol{k}, \qquad \tau = \varrho t, \tag{48}$$

where $\tilde{j}_n(\boldsymbol{k}, \tau)$ is a slow modulation of the time harmonic carrier waves. We also set the currents to vanish for negative times, i.e.

$$\boldsymbol{J}(\boldsymbol{r}, t) = \boldsymbol{0}, \qquad \tilde{j}_n(\boldsymbol{k}, \varrho t) = 0 \qquad \text{if } t \leqslant 0. \tag{49}$$

Then we recast the fields $\boldsymbol{U}(\boldsymbol{r}, t)$ and the corresponding equations in terms of the fields $\boldsymbol{V}^{(0)}(\tau)$ and $\boldsymbol{V}^{(1)}(\tau)$ introduced in the previous section. In the linear case, $\alpha = 0$, when $\boldsymbol{J}$ is defined by (48) and (49), the modal form of the solution $\boldsymbol{V}^{(0)}$ to the Maxwell equations (15) is

$$\tilde{V}_{\bar{n}}^{(0)}(\boldsymbol{k}, \tau) = -\int_0^\tau \tilde{j}_{\bar{n}}(\boldsymbol{k}, \tau_1)\, \mathrm{d}\tau_1. \tag{50}$$

To describe the modal expansion of the first nonlinear response $\tilde{V}_{\bar{n}}^{(1)}(\boldsymbol{k}, \tau)$ we introduce triads of eigenmodes $(\bar{n}, \boldsymbol{k})$, $(\bar{n}', \boldsymbol{k}')$ and $(\bar{n}'', \boldsymbol{k}'')$ satisfying the *phase matching condition*

$$\boldsymbol{k}'' = \boldsymbol{k} - \boldsymbol{k}'. \tag{51}$$

Then we introduce the following *phase function*:

$$\phi_{\vec{n}}(\boldsymbol{k}, \boldsymbol{k}') = \omega_{\bar{n}}(\boldsymbol{k}) - \omega_{\bar{n}'}(\boldsymbol{k}') - \omega_{\bar{n}''}(\boldsymbol{k} - \boldsymbol{k}'), \qquad \vec{n} = (\bar{n}, \bar{n}', \bar{n}''), \tag{52}$$

playing a decisive role in the nonlinear mode interactions. The Bloch modal form of the first nonlinear response (30) is

$$\tilde{V}_{\bar{n}}^{(1)}(\boldsymbol{k}, \tau) = \frac{\alpha}{\varrho} \sum_{\bar{n}', \bar{n}''} \int_0^\tau \mathcal{I}(\tilde{V}^{(0)} | \vec{n}, \boldsymbol{k}, \tau_1)\, \mathrm{d}\tau_1, \tag{53}$$

$$\mathcal{I}(\tilde{V}^{(0)} | \vec{n}, \boldsymbol{k}, \tau_1) = \int_{[-\pi,\pi]^3} \mathrm{e}^{\mathrm{i}\phi_{\vec{n}}(\boldsymbol{k},\boldsymbol{k}')\tau_1/\varrho} \tilde{Q}_{\vec{n}}[\tilde{V}^{(0)} | \vec{n}, \boldsymbol{k}, \boldsymbol{k}', \tau_1]\, \mathrm{d}\boldsymbol{k}', \tag{54}$$

$$\tilde{Q}_{\vec{n}}[\tilde{V}^{(0)} | \vec{n}, \boldsymbol{k}, \boldsymbol{k}', \tau_1] = \breve{Q}_{\vec{n}} \tilde{V}_{\bar{n}'}^{(0)}(\boldsymbol{k}', \tau_1) \tilde{V}_{\bar{n}''}^{(0)}(\boldsymbol{k} - \boldsymbol{k}', \tau_1), \tag{55}$$

where $\breve{Q}_{\vec{n}}$ is a coefficient depending on $\boldsymbol{k}$ and $\boldsymbol{k}'$ (see [12] for detail).

Let us now look at formulae (53), (54) accounting for the nonlinear mode interactions. The time derivative $\mathrm{d}\tilde{V}_{\bar{n}}^{(1)}(\boldsymbol{k}, \tau)/\mathrm{d}\tau$ is proportional to the sum of the quantities $\mathcal{I}(\tilde{V}^{(0)} | \vec{n}, \boldsymbol{k}, \tau_1)$ each of which can be naturally interpreted as an interactive contribution of the $(\bar{n}', \boldsymbol{k}')$ and $(\bar{n}'', \boldsymbol{k} - \boldsymbol{k}')$ components of the linear wave $\tilde{V}^{(0)}$ to the $(\bar{n}, \boldsymbol{k})$ component of the first nonlinear response $\tilde{V}_{\bar{n}}^{(1)}$. For this reason we refer to the integrals $\mathcal{I}(\tilde{V}^{(0)} | \vec{n}, \boldsymbol{k}, \tau_1)$ in (54) as the *oscillatory interaction integrals*.

3. Selection rules for stronger nonlinear interactions

To take advantage of the representation (53), (54) for the analytical studies of the nonlinear phenomena, we consider the asymptotic behaviour of the interaction integrals $\mathcal{I}$ for $\varrho \ll 1$. In other worlds, we consider the first nonlinear response of the medium to almost harmonic fields of infinitesimally small amplitudes.

Note that the interaction integral $\mathcal{I}$ defined by (54) has a factor $\mathrm{e}^{\mathrm{i}\phi_{\vec{n}}(\boldsymbol{k},\boldsymbol{k}')\frac{\tau_1}{\varrho}}$ rapidly oscillating as $\varrho \to 0$. *It is this factor that ultimately, determines which modes in the right-hand side of* (53) *produce substantial contributions to* $\tilde{V}_{\bar{n}}^{(1)}$. Let us look now at the *selection rules* allowing us to single out stronger interacting modes.

It follows from (53), (54) that the modes for which the phase

$$\phi_{\vec{n}}(\boldsymbol{k}, \boldsymbol{k}', \boldsymbol{k}'') = \omega_{\bar{n}}(\boldsymbol{k}) - \omega_{\bar{n}'}(\boldsymbol{k}') - \omega_{\bar{n}''}(\boldsymbol{k} - \boldsymbol{k}') \tag{56}$$

vanishes would give larger contributions to $\tilde{V}_{\bar{n}}^{(1)}$ than those for which it does not. This yields the first selection rule known as the *FMC or sum-frequency mixing condition* [16, 17, 47],

$$\omega_{\bar{n}}(\boldsymbol{k}) - \omega_{\bar{n}'}(\boldsymbol{k}') - \omega_{\bar{n}''}(\boldsymbol{k} - \boldsymbol{k}') = 0. \tag{57}$$

We can further narrow down the set of stronger interacting modes by applying the *stationary phase method* [7, 26, 28, 29, 32, 51], to the integral (54). According to the method, the asymptotic approximation to the oscillatory integral (54) as $\varrho \to 0$ is determined by infinitesimally small vicinities of the critical points $\boldsymbol{k}'_*$ satisfying the following equation:

$$\nabla_{\boldsymbol{k}'}\phi_{\vec{n}}(\boldsymbol{k},\boldsymbol{k}'_*) = 0. \tag{58}$$

For the phase function ϕ defined by (56) equation (58) reduces to

$$\nabla\omega_{\bar{n}'}(\boldsymbol{k}'_*) = \nabla\omega_{\bar{n}''}(\boldsymbol{k}-\boldsymbol{k}'_*). \tag{59}$$

Since $\nabla\omega(\boldsymbol{k})$ is the group velocity, the selection rule (59) is naturally interpreted as the *GVC*, and can be viewed as a selection rule for modes of stronger interaction. We show in section 5 that the group velocity $\boldsymbol{v}_{\mathrm{gr}}(\boldsymbol{V}^{(1)}_{\bar{n},\boldsymbol{k}})$ of the first nonlinear response matches exactly the group velocities in (59) [12], i.e.

$$\boldsymbol{v}_{\mathrm{gr}}(\boldsymbol{V}^{(1)}_{\bar{n},\boldsymbol{k}}) = \nabla\omega_{\bar{n}'}(\boldsymbol{k}'_*) = \nabla\omega_{\bar{n}''}(\boldsymbol{k}-\boldsymbol{k}'_*). \tag{60}$$

Note that the group velocity (60) *of the first nonlinear response* $\tilde{V}^{(1)}_{\bar{n}}(\boldsymbol{k},\tau)$ *related to the* $(\bar{n},\boldsymbol{k})$*-mode differs from the group velocity* $\nabla\omega_{\bar{n}}(\boldsymbol{k})$ *of same mode as a linear wave!*

As to the known *phase matching condition* $\boldsymbol{k} = \boldsymbol{k}' + \boldsymbol{k}''$, see (51), observe that it is already explicitly taken into account when we introduced the interaction integrals $\mathcal{I}(\tilde{V}^{(0)}|\,\vec{n},\boldsymbol{k},\tau_1)$ by (54), (see [12] for details).

For a given $(\bar{n},\boldsymbol{k})$ let us denote the values of the vector $\boldsymbol{k}'$ and indices $\bar{n}'$, $\bar{n}''$ satisfying the matching conditions (57) and (59) by respectively $\boldsymbol{k}'_{*l}$ and $\bar{n}'_l$, $\bar{n}''_l$, where the index l numerates points satisfying the selection rules. The interaction integrals $\mathcal{I}(\tilde{V}^{(0)}|\,\vec{n},\boldsymbol{k},\tau_1)$ in (53) as $\varrho \to 0$ are essentially determined by infinitesimally small vicinities of the points $\boldsymbol{k}'_{*l}$, and their contributions to $\tilde{V}^{(1)}_{\bar{n}}(\boldsymbol{k},\tau)$ are of the form, [12],

$$\frac{\alpha}{\varrho}B_l(\boldsymbol{k},\tau)\varrho^{q(\boldsymbol{k},\boldsymbol{k}'_{*l})}(1+o_{\varrho}(1)) \qquad \text{where } q(\boldsymbol{k},\boldsymbol{k}'_{*l}) > 0, \tag{61}$$

and

$$B_l(\boldsymbol{k},\tau) = \int_0^{\tau} \bar{Q}_{\vec{n}_l}[\tilde{V}^{(0)}|\,\boldsymbol{k},\boldsymbol{k}'_{*l},\tau_1]\,\mathrm{d}\tau_1, \qquad \vec{n}_l = (\bar{n},\bar{n}'_l,\bar{n}''_l).$$

The *interaction index* $q(\boldsymbol{k},\boldsymbol{k}'_{*l})$ in formula (61) determines the relative strength of the impact of the modes $(\bar{n}'_l,\boldsymbol{k}'_{*l})$ and $(\bar{n}''_l,\boldsymbol{k}''_{*l})$, with $\boldsymbol{k}''_{*l} = \boldsymbol{k}-\boldsymbol{k}'_{*l}$, on the mode $(\bar{n},\boldsymbol{k})$ as a result of the nonlinear interaction. As a consequence, we also get from (53) the following asymptotic formula:

$$\tilde{V}^{(1)}_{\bar{n}}(\boldsymbol{k},\tau) = \frac{\alpha}{\varrho}\sum_l B_l(\boldsymbol{k},\tau)\varrho^{q(\boldsymbol{k},\boldsymbol{k}'_{*l})}(1+o_{\varrho}(1)), \qquad \varrho \to 0. \tag{62}$$

Formula (62) can be simplified if we introduce the *leading interaction index*

$$q_0(\boldsymbol{k}) = \min_l q(\boldsymbol{k},\boldsymbol{k}'_{*l}), \tag{63}$$

and the set $L_{\boldsymbol{k}}$ of all l for which the minimum is attained, i.e.

$$L_{\boldsymbol{k}} = \{l : q(\boldsymbol{k},\boldsymbol{k}'_{*l}) = q_0(\boldsymbol{k})\}. \tag{64}$$

Denoting

$$B(\boldsymbol{k},\tau) = \sum_{l\in L_{\boldsymbol{k}}} B_l(\boldsymbol{k},\tau) \tag{65}$$

we get from (62) the following asymptotic representation of the first nonlinear response:

$$\tilde{V}^{(1)}_{\bar{n}}(\boldsymbol{k},\tau) = \frac{\alpha}{\varrho}B(\boldsymbol{k},\tau)\varrho^{q_0(\boldsymbol{k})}(1+o_{\varrho}(1)), \qquad \varrho \to 0. \tag{66}$$

We would like to remark that *the GVC stemming from stationary phase condition* (58) *is, in fact, the most important selection rule*. Indeed, it follows from the stationary phase method that if (58) does not hold, then the corresponding oscillatory integral will decay faster than any positive power ϱ^N as $\varrho \to 0$. In other words, the failure to comply with the group velocity condition sets the interaction index q_0 to be infinite, indicating the weakest nonlinear interaction. In contrast, if the FMC (57) does not hold, that would lift the interaction index q_0 by 1 (see section 7 and table 2). In the case of an ideal dispersionless homogeneous medium the GVC is obscured since it coincides exactly with the phase matching condition (51) for $\omega_{\bar{n}}(\boldsymbol{k}) = \text{constant}\,|\boldsymbol{k}|$.

The significance of the GVC for nonlinear interactions have been pointed out in a number of papers [19, 35, 43, 55, 57]. In [12] and in this paper we show that the GVC is an asymptotically exact selection rule following consistently from the stationary phase principle for nonlinear regimes satisfying the constraints imposed in the introduction and also discussed in the following section.

It is also worthy of note that the interaction index q_0 senses roughly how many modes are involved in the nonlinear interaction. In other words, the interaction index q_0 can be smaller, indicating stronger interaction, when the density of interacting modes approaches infinity at a higher rate. The nonlinear interaction enhancement for the second and third harmonic generation due to to larger density of modes in a known phenomenon, see, for instance [18, 23] and references therein.

3.1. Limitations related to the stationary phase method

When applying the stationary phase method in the analysis of interaction integrals in (53), (54) we assume the smoothness, i.e. the differentiability, of the amplitude $\tilde{Q}_{\bar{n}}[\tilde{V}^{(0)}|\,\boldsymbol{k}, \boldsymbol{k}', \tau_1]$ as a function of the quasimomentum $\boldsymbol{k}'$. In view of (50), the condition ultimately reduces to the smoothness in $\boldsymbol{k}$ of the Floquet–Bloch transform $\tilde{j}_{\bar{n}}(\boldsymbol{k}, \tau_1)$ of the excitation currents. This is a physically significant assumption affecting the spatial range of the wave in the form of constraint (31). To expose this relation we give the following general definition of the spatial range of a wave.

First, we introduce a normalized wavefunction $\boldsymbol{\Phi}(\boldsymbol{r})$, i.e. $\int |\boldsymbol{\Phi}(\boldsymbol{r})|^2\,\mathrm{d}\boldsymbol{r} = 1$ (for instance, the wavefunction corresponding to the excitation currents). Then we introduce for an observable physical quantity ξ (a linear self-adjoint operator), its average (expected value) and the mean-square deviation in the state $\boldsymbol{\Phi}$ respectively, using (see, for instance [46], sections 7, 12)

$$\langle \xi \rangle_{\boldsymbol{\Phi}} = \int \boldsymbol{\Phi}^*(\boldsymbol{r})\xi\boldsymbol{\Phi}(\boldsymbol{r})\,\mathrm{d}\boldsymbol{r}, \qquad (\boldsymbol{\Delta}\xi_{\boldsymbol{\Phi}})^2 = \langle(\xi - \langle\xi\rangle_{\boldsymbol{\Phi}})^2\rangle_{\boldsymbol{\Phi}}. \tag{67}$$

In particular, let $\boldsymbol{r} = (r_1, \ldots, r_d)$ be the position operator; $[\boldsymbol{r}]$ is its integer-valued part. In other words, $[\boldsymbol{r}]$ determines in which cell the point $\boldsymbol{r}$ resides. Then we have

$$([\boldsymbol{\Delta}[r]_j]_{\boldsymbol{\Phi}})^2 = \langle([r]_j - \langle[r]_j\rangle_{\boldsymbol{\Phi}})^2\rangle_{\boldsymbol{\Phi}}, \qquad j = 1, 2, 3. \tag{68}$$

Note that $\langle[r]_j\rangle_{\boldsymbol{\Phi}}$ are the integer-valued coordinates of the wave centre. We define now the spatial range $L_{\boldsymbol{\Phi}}$ of the wave $\boldsymbol{\Phi}(\boldsymbol{r})$ by the formula

$$L_{\boldsymbol{\Phi}}^2 = \sum_{j=1}^{3} \langle([r]_j - \langle[r]_j\rangle_{\boldsymbol{\Phi}})^2\rangle_{\boldsymbol{\Phi}}. \tag{69}$$

Denoting $\tilde{\boldsymbol{\Phi}} = \{\tilde{\boldsymbol{\Phi}}_{\bar{n}}(\boldsymbol{k})\}$ the Floquet–Bloch transform (46) of $\boldsymbol{\Phi}(\boldsymbol{r})$ and using its basic properties (see [12], section 5.1) we get

$$\langle [r]_j \rangle_{\Phi} = \int_{R^d} \Phi^*(r)[r]_j \Phi(r)\, dr = \frac{1}{(2\pi)^d} \sum_{\vec{n}} \int_{[-\pi,\pi]^3} \tilde{\Phi}^*_{\vec{n}}(k) \partial_{k_j} \tilde{\Phi}_{\vec{n}}(k)\, dk = \langle \partial_{k_j} \rangle_{\tilde{\Phi}}, \tag{70}$$

and

$$\langle ([r]_j - \langle [r]_j \rangle_{\Phi})^2 \rangle_{\Phi} = \frac{1}{(2\pi)^d} \langle (\partial_{k_j} - \langle \partial_{k_j} \rangle_{\tilde{\Phi}})^2 \rangle_{\tilde{\Phi}}. \tag{71}$$

Now summing up the expressions in (71) over j and using (67)–(69) we obtain the following identity

$$L^2_{\Phi} = \frac{1}{(2\pi)^d} \sum_{\vec{n}} \int_{[-\pi,\pi]^3} (\nabla_k \tilde{\Phi}^*_{\vec{n}}(k) - \langle \nabla_k \rangle_{\tilde{\Phi}})^2\, dk \tag{72}$$

directly relating the mean-square average of the derivative $\tilde{\Phi}$ in k to the spatial range of the wave.

Therefore, based on (72) we can conclude that the assumption of the smoothness of $\tilde{\Phi}$ in k is, in fact, directly related to the spatial range $L_{\Phi} = L_{\mathrm{wp}}$ of the wave Φ. Since we consider infinite photonic crystals, i.e. $L_{\mathrm{phcryst}} = \infty$, the requirement of smoothness of $\tilde{\Phi}$ in k reduces to $L_{\Phi} = L_{\mathrm{wp}} < \infty$. In the case of a finite L_{phcryst} the appropriate condition would be $L_{\mathrm{wp}} \ll L_{\mathrm{phcryst}}$ as in (31).

When the stationary phase method is applicable it yields (see (58) and (59)) the group velocity matching as a selection rule. We have shown in [12] and in the following sections that in the important case of the SHG the group velocity matching is satisfied for appropriate triads of modes. In a number of situations, when the group velocity matching does not hold automatically, such as in the process of parametric soliton generation, its significance is well known in physical literature (see [19, 35, 43, 55, 57]). In particular, the results of [19] show that a group-velocity mismatch prevents spatial soliton formation.

In situations when the constraints described in the introduction, in particular, (31), are not satisfied, our conclusions on the relative significance of different selection rules might not hold. For instance, in [48] the periodic structure is many times smaller than the pulse spatial range, that is $L_{\mathrm{wp}} \gg L_{\mathrm{phcryst}}$. Consequently, the features of nonlinear regimes are substantially different.

4. Analytic properties of the dispersion relations and the phases

To study and classify the nonlinear interactions, we have to first investigate the analytic properties of the dispersion relations $\omega_n(k)$ and, consequently, the phases $\phi_{\vec{n}}(k, k')$ defined by (52), since they play a significant role in the analysis of the interaction integrals $\mathcal{I}(\tilde{V}^{(0)} | \vec{n}, k, \tau_1)$ in (54). Consequently this section is devoted to the consideration of mathematical concepts needed for the analysis of the interaction integrals related to the first nonlinear response.

It is shown in section 3 that the modes described by k and k'_* will have a stronger nonlinear interaction only if they satisfy the stationary phase (group velocity matching) condition

$$\nabla_{k'} \phi_{\vec{n}}(k, k'_*) = -\nabla \omega_{\vec{n}'}(k'_*) + \nabla \omega_{\vec{n}''}(k - k'_*) = \mathbf{0}. \tag{73}$$

The points k'_* satisfying (73) are called *critical*. In the case when the phase $\phi_{\vec{n}}(k, k')$ is differentiable at k'_* we shall call a point k'_* satisfying (73) a *simple critical point*.

In the case when both k'_* and $k''_* = k - k'_*$ are such that the respective multiplicities of the eigenvalues $\omega_{\vec{n}'}(k'_*)$ and $\omega_{\vec{n}''}(k - k'_*)$ are exactly one, then the phase $\phi_{\vec{n}}(k, k')$ is differentiable at $k' = k'_*$. Consequently, gradients of the eigenfrequencies are well defined, and equation (73) has a straightforward interpretation as the GVC.

If $\boldsymbol{k}'_*$ is the simple critical point satisfying (73) then, according to the classical theory of oscillatory integrals, the order of asymptotic approximation of the interaction integral $\mathcal{I}(\tilde{V}^{(0)} | \vec{n}, \boldsymbol{k}, \tau_1)$, defined by (54), depends on whether the Hessian $\{\nabla^2_{\boldsymbol{k}'}\phi_{\vec{n}}(\boldsymbol{k}, \boldsymbol{k}'_*)\}$ of the phase is non-degenerate, i.e. if the matrix $\{\nabla^2_{\boldsymbol{k}'}\phi_{\vec{n}}(\boldsymbol{k}, \boldsymbol{k}'_*)\}$ has the maximal rank which is d, where d is the space dimension. Evidently, the non-degenerate case can be also identified by the condition

$$\det\{\nabla^2_{\boldsymbol{k}'}\phi_{\vec{n}}(\boldsymbol{k}, \boldsymbol{k}'_*)\} \neq 0. \qquad (74)$$

If (74) holds we call $\boldsymbol{k}'_*$ a non-degenerate *critical point*. The contribution of non-degenerate critical points to the oscillatory integrals is given by the well known classical asymptotic formula [51] (section VIII, 2.3.2), [7] (theorem 6.2) [28, 29]).

If the rank of the Hessian $\{\nabla^2_{\boldsymbol{k}'}\phi_{\vec{n}}(\boldsymbol{k}, \boldsymbol{k}')\}$ is smaller than d and, consequently

$$\det\{\nabla^2_{\boldsymbol{k}'}\phi_{\vec{n}}(\boldsymbol{k}, \boldsymbol{k}'_*)\} = 0,$$

we call the point $\boldsymbol{k}'_*$ a *degenerate critical point*. A general qualitative result describing the asymptotics of oscillatory integrals in $\boldsymbol{R}^d$ for degenerate critical points is presented in [7] (theorem 6.3), [51] (section VIII, 5.5).

If the phase is not differentiable, the asymptotic analysis is more complicated. It must be noted that the issue of differentiability of the functions $\omega_n(\boldsymbol{k})$ is far from trivial, [39] (sections II.5, II.7), especially for the space dimensions $d = 2, 3$. The problem of non-differentiability is caused by multiple eigenvalues. The multiplicity of eigenvalues of differential operators and their dependence on parameters are the subjects of extensive studies (see, for instance [38, 39, 56, 59] and [5] (appendix 10, p 425), for detailed discussions of the dependence of eigenvalues on parameters).

In the one-dimensional case $d = 1$ generically there is no problem with differentiability. Thus, it remains to study the cases $d = 2, 3$. Fortunately, in our problems it is sufficient to consider only the multiplicity 2 [12].

4.1. Band-crossing points for the space dimension $d = 2$

We call a point $\boldsymbol{k}_\otimes = (k_{\otimes 1}, k_{\otimes 2})$ a *band crossing point* (BC point) if there exists n such that $\omega_n(\boldsymbol{k}_\otimes) = \omega_{n+1}(\boldsymbol{k}_\otimes)$. In the two-dimensional case $d = 2$ in a generic situation there is a finite number of BC points $\boldsymbol{k}_\otimes$. Analysis shows that the sum $\omega_n(\boldsymbol{k}) + \omega_{n+1}(\boldsymbol{k})$ is always analytic in the vicinity of $\boldsymbol{k}_\otimes$ whereas the difference $\omega_n(\boldsymbol{k}) - \omega_{n+1}(\boldsymbol{k})$ is non-differentiable at $\boldsymbol{k}_\otimes$. The typical behaviour of the functions $\omega_n(\boldsymbol{k}_\otimes)$ and $\omega_{n+1}(\boldsymbol{k}_\otimes)$ in the vicinity of a BC point $\boldsymbol{k}_\otimes$ is depicted in figure 2.

It turns out that after a proper local change of variables $\boldsymbol{k}$ in a vicinity of $\boldsymbol{k}_\otimes$ the functions $\omega_n(\boldsymbol{k})$ and $\omega_{n+1}(\boldsymbol{k})$ become analytic in new variables. These new variables can be defined as a composition of a linear map and generalized polar variables r, θ, namely

$$k_1 = k_{\otimes 1} + a_1 r \cos(\theta - \theta_0), \qquad k_2 = k_{\otimes 2} + a_2 r \sin\theta, \qquad (75)$$

where constants a_1, a_2 and $\theta_0 \neq \pm\pi/2$ depend on $\boldsymbol{k}_\otimes$. The functions $\omega_n(\boldsymbol{k})$ and $\omega_{n+1}(\boldsymbol{k})$ are analytic functions of r and θ (see [12] for more details).

Let now $\varphi(\boldsymbol{k})$ stand for either of functions $\omega_n(\boldsymbol{k})$, $\omega_{n+1}(\boldsymbol{k})$ or for the phase $\phi_{\vec{n}}(\boldsymbol{k}, \boldsymbol{k}')$. A thorough analysis based on the results in [12] (section 5.4), show that for properly chosen a_1, a_2 and θ_0 the following representation holds in a vicinity of a BC point $\boldsymbol{k}_\otimes$

$$\varphi(\boldsymbol{k}) = \varphi(\boldsymbol{k}_\otimes) + \psi(\boldsymbol{k}) + r\left[\cos(\theta_0) + \sum_{j=1}^{\infty} b_j(\theta) r^j\right], \qquad r \ll 1, \qquad (76)$$

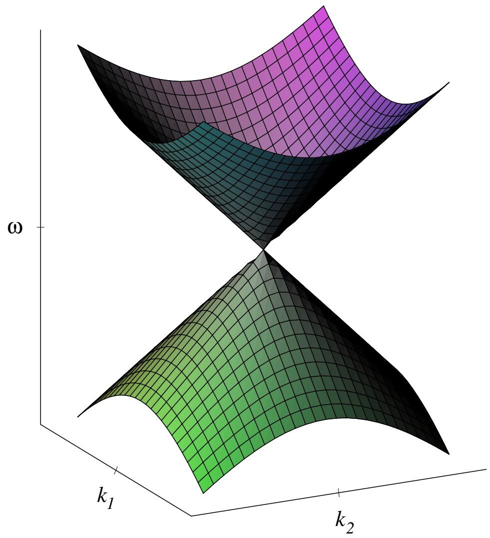

Figure 2. In the two-dimensional case $d = 2$ two branches of eigenvalues at a BC point typically form a conical surface as it is shown in the figure. Remarkably, the intersection is a point, and not a curve! Another remarkable phenomenon is that the conical intersection for two eigenvalue surfaces is robust and it continues to hold under small self-adjoint perturbations of the related operators.

where $\psi(\boldsymbol{k})$ is an analytic in $\boldsymbol{k}$ function, and $b_j(\theta)$ are smooth 2π-periodic functions of θ. It can also be shown that there exists a smooth local change of variables

$$r, \theta \to \tilde{r}, \tilde{\theta} \tag{77}$$

such that yields the following canonical representation for the phase:

$$\varphi(\boldsymbol{k}) = \varphi(\boldsymbol{k}_\otimes) + \psi(\tilde{r}\cos\tilde{\theta}, \tilde{r}\sin\tilde{\theta}) + \tilde{r} \tag{78}$$

where ψ is analytic. This exact phase representation plays the key role in the rigorous analysis of the asymptotic approximation of the oscillatory integral

$$I_\delta(\boldsymbol{k}_\otimes) = \int_{|\boldsymbol{k}-\boldsymbol{k}_\otimes|\leqslant\delta} \mathrm{e}^{\mathrm{i}\varphi(\boldsymbol{k})\tau/\varrho} A(\boldsymbol{k})\,\mathrm{d}\boldsymbol{k} = \int_0^\delta r\,\mathrm{d}r \int_0^{2\pi} \mathrm{e}^{\mathrm{i}\varphi(r,\theta)\tau/\varrho} A(r,\theta)\,\mathrm{d}\theta. \tag{79}$$

The gradient $\nabla_{\boldsymbol{k}}\varphi(\boldsymbol{k})$ is not continuous at the BC point $\boldsymbol{k}_\otimes$. The typical behaviour of $\nabla_{\boldsymbol{k}}\varphi(\boldsymbol{k})$ near $\boldsymbol{k}_\otimes$ is similar to $(\boldsymbol{k}-\boldsymbol{k}_\otimes)/|\boldsymbol{k}-\boldsymbol{k}_\otimes|$, that can be looked at as a situation when the gradient takes on infinitely many values. Let us show that the generalized polar coordinates (75) allow one to give meaning to the multiple-valued gradient $\nabla_{\boldsymbol{k}}\varphi(\boldsymbol{k})$ at a BC point $\boldsymbol{k}_\otimes$. Indeed, note that $\nabla_{\boldsymbol{k}}\varphi$ takes the following form in oblique polar coordinates (75):

$$\nabla_{\boldsymbol{k}}\varphi = \nabla_{\boldsymbol{k}}\psi(\boldsymbol{k}) + ([\nabla_{\boldsymbol{k}}(\varphi-\psi)]_1, [\nabla_{\boldsymbol{k}}(\varphi-\psi)]_2) \tag{80}$$

$$[\nabla_{\boldsymbol{k}}(\varphi-\psi)]_1 = \frac{\cos\theta\, r\,\partial_r(\varphi-\psi) - \sin\theta\,\partial_\theta(\varphi-\psi)}{a_1 r\cos\theta_0} \tag{81}$$

$$[\nabla_{\boldsymbol{k}}(\varphi-\psi)]_2 = \frac{r\sin(\theta-\theta_0)\partial_r(\varphi-\psi) + \cos(\theta-\theta_0)\partial_\theta(\varphi-\psi)}{a_2 r\cos\theta_0} \tag{82}$$

and, hence,

$$[\nabla_{\boldsymbol{k}}\varphi(\boldsymbol{k}_\otimes)] = \lim_{r\to 0}\nabla_{\boldsymbol{k}}\varphi(\boldsymbol{k}_\otimes) = [[\nabla_{\boldsymbol{k}}\varphi(\boldsymbol{k}_\otimes)]_1, [\nabla_{\boldsymbol{k}}\varphi(\boldsymbol{k}_\otimes)]_2] \tag{83}$$

$$[\nabla_{\boldsymbol{k}}\varphi(\boldsymbol{k}_\otimes)]_1 = [\psi(\boldsymbol{k}_\otimes)]_1 + \left.\frac{\cos\theta\,\partial_r(\varphi-\psi) - \sin\theta\,\partial_\theta\partial_r(\varphi-\psi)}{a_1\cos\theta_0}\right|_{r=0} \tag{84}$$

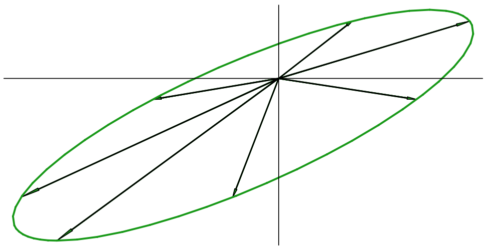

Figure 3. The figure shows all the values of the gradient of a phase φ at a BC point $\boldsymbol{k}_\otimes$. The typical elliptic curve is spanned by the tip of the gradient $\nabla_{\boldsymbol{k}}\varphi(\boldsymbol{k}_\otimes)$ as θ runs from 0 to 2π. The arrows indicate the gradient for several values of θ. In this particular case the gradient has all the directions between 0 and 2π with every direction occurring exactly once.

$$[\nabla_{\boldsymbol{k}}\varphi(\boldsymbol{k}_\otimes)]_2 = [\psi(\boldsymbol{k}_\otimes)]_2 + \left.\frac{\sin(\theta-\theta_0)\partial_r\varphi + \cos(\theta-\theta_0)\partial_\theta\partial_r\varphi}{a_2\cos\theta_0}\right|_{r=0}. \tag{85}$$

In particular, for $\varphi(\boldsymbol{k})$ defined by (75), (76) we get

$$\nabla_{\boldsymbol{k}}\varphi(\boldsymbol{k}_\otimes) = \nabla_{\boldsymbol{k}}\varphi(\boldsymbol{k}_\otimes,\theta) = \nabla_{\boldsymbol{k}}\psi(\boldsymbol{k}_\otimes) + \left[\frac{\cos\theta}{a_1}, \frac{\sin(\theta-\theta_0)}{a_2}\right], \qquad 0 \leqslant \theta \leqslant 2\pi. \tag{86}$$

Observe, that the formula (86) indicates that the gradient at a BC point $\boldsymbol{k}_\otimes$ is the sum of the two terms: the first one is a regular analytic $\nabla_{\boldsymbol{k}}\psi(\boldsymbol{k}_\otimes)$, whereas the second one has multiple values as the angle θ varies.

Formula (83) holds for functions φ which are not differentiable in Cartesian coordinates but are twice differentiable in the polar coordinates, as our dispersion relations and phases are at BC points. Observe also that $\nabla_{\boldsymbol{k}}\varphi(\boldsymbol{k}_\otimes)$ defined by (83), (86) becomes a function of the angle θ which naturally reflects the phenomenon of multiple values of the gradient at a BC point.

A rather laborious analysis of the integrals (79) shows that the dominant contribution to the integrals for $\varrho \to 0$ is proportional to $\varrho^{\frac{5}{4}}$. Note that the similar integral with $\boldsymbol{k}$ being a simple non-degenerate critical point would be asymptotically proportional to ϱ, which is the value of $\varrho^{\frac{d}{2}}$ for $d = 2$.

In the two-dimensional case $d = 2$ generically there will be at most a finite number of BC points. For every such point there exists its vicinity in which the eigenvalues and the eigenvectors are analytic functions in the polar coordinates.

Figures 3–5 show several typical examples of the multiple valued gradient at a BC point.

4.2. Band-crossing points for the space dimension $d = 3$

In the case $d = 3$ the BC points $\boldsymbol{k}_\otimes$ related to $\omega_n(\boldsymbol{k})$ form smooth *band-crossing curves* [12]. Let us consider one of those curves $\Gamma_\otimes$ and pick a point $\boldsymbol{k}_\otimes$ in $\Gamma_\otimes$. Let $\boldsymbol{\xi}(\boldsymbol{k}_\otimes)$ and $\Xi(\boldsymbol{k}_\otimes)$ be respectively the tangent vector to the curve $\Gamma_\otimes$ at the point $\boldsymbol{k}_\otimes$ and the plane passing through $\boldsymbol{k}_\otimes$ and perpendicular to $\boldsymbol{\xi}(\boldsymbol{k}_\otimes)$. It turns out that in a generic case the function $\omega_n(\boldsymbol{k})$ is differentiable in the direction $\boldsymbol{\xi}(\boldsymbol{k}_\otimes)$ and, hence, the tangential derivative $\nabla\omega_n(\boldsymbol{k}_\otimes)\cdot\boldsymbol{\xi}(\boldsymbol{k}_\otimes)$ is well defined. As to the behaviour of $\omega_n(\boldsymbol{k})$ in the plane $\Xi(\boldsymbol{k}_\otimes)$ it is similar to the case of BC points for the space dimension $d = 2$. In other words, the function $\omega_n(\boldsymbol{k})$ is an analytic function in an appropriately chosen curvilinear cylindrical coordinate system. The typical behaviour of the multiple valued gradient at a BC point is shown in figure 6.

Let us consider now the BC points $\boldsymbol{k}_\otimes$ related to the phase $\phi_{\vec{n}}(\boldsymbol{k},\boldsymbol{k}')$ and belonging to one of the band-crossing curves $\Gamma_\otimes$. The most significant contributions to the interaction integral

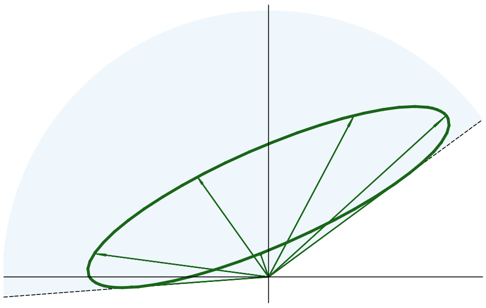

Figure 4. Here we give another example of the gradient at a BC point $\boldsymbol{k}_\otimes$. The elliptic curve is spanned by the tip of the gradient $\nabla_{\boldsymbol{k}}\varphi(\boldsymbol{k}_\otimes)$ as θ runs from 0 to 2π, with arrows indicating its values. The shadowed area indicates a sector of allowed directions for the gradient with every direction, except for the extreme, occurring twice as θ runs from 0 to 2π.

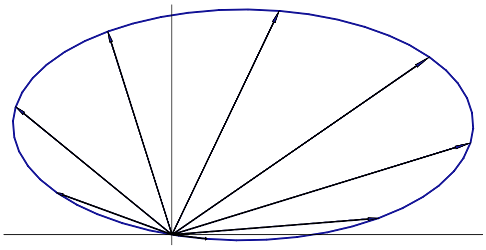

Figure 5. This is an example of the gradient at BC point $\boldsymbol{k}_\otimes$ which takes on $\mathbf{0}$. The elliptic curve is spanned by the tip of the gradient $\nabla_{\boldsymbol{k}}\varphi(\boldsymbol{k}_\otimes)$ as θ runs from 0 to 2π. The arrows indicate several values of the gradient. Every direction, except for one, occurs exactly once.

come from points on $\Gamma_\otimes$ at which the tangential derivative of $\phi_{\vec{n}}(\boldsymbol{k}, \boldsymbol{k}'_\otimes)$ vanishes, i.e.

$$\nabla\phi_{\vec{n}}(\boldsymbol{k}, \boldsymbol{k}'_\otimes) \cdot \boldsymbol{\xi}(\boldsymbol{k}, \boldsymbol{k}'_\otimes) = 0. \tag{87}$$

In the three-dimensional case $d = 3$ generically there will be at most a finite number of band-crossing curves. The stationary phase (group velocity matching) condition (87) will generally select a finite number of modes with the strongest nonlinear interaction.

5. The group velocity and nonlinear interactions

As we have already pointed out the *group velocity condition is the most important, and, in fact, a necessary condition for stronger nonlinear interaction for the regimes under study*. If the condition does not hold, the relevant interaction integral has infinite index and, hence, decays faster than any positive power of ϱ as $\varrho \to 0$. In this section we study in detail the issues related to the GVC.

5.1. The group velocity of the first nonlinear response

To find the group velocity of the first nonlinear response $\tilde{V}^{(1)}_{\vec{n}}(\boldsymbol{k}, \tau)$, considering it as a wave on its own, we recall, first, the derivation of the representation of the group velocity in a periodic medium. The group velocity can be found in the case of homogeneous media by the stationary phase method [61] (section 11.4), [32] (section 1.6a). The same approach can also be used for

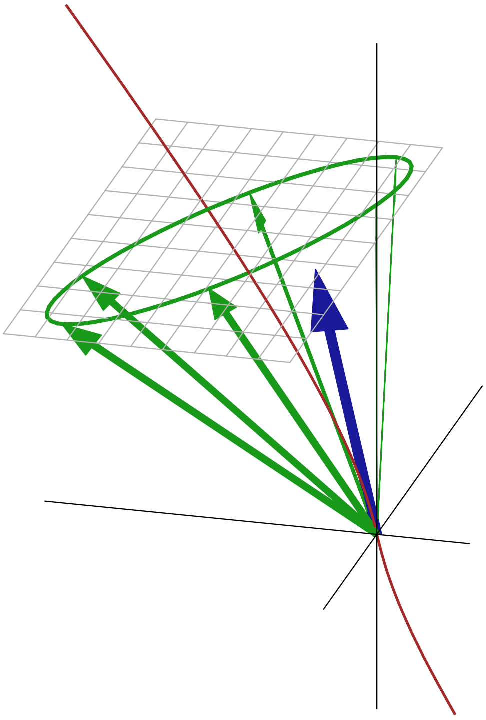

Figure 6. This is an example of the gradient at a BC point $\boldsymbol{k}_{\otimes}$ (shown as the origin) for three-dimensional space. The solid thinner curve is a curve $\Gamma_{\otimes}$ of BC points including $\boldsymbol{k}_{\otimes}$. The elliptic curve is spanned by the tip of the gradient $\nabla_{\boldsymbol{k}}\varphi(\boldsymbol{k}_{\otimes})$ as θ runs from 0 to 2π. The thinner arrows indicate several values of the multiple-valued gradient. The bolder arrow, at a tangent to the curve of BC points $\Gamma_{\otimes}$, describes the tangential component of the gradient parallel to $\boldsymbol{\xi}(\boldsymbol{k}_{\otimes})$. The phase is always differentiable in the direction $\boldsymbol{\xi}(\boldsymbol{k}_{\otimes})$. The most significant contributions to the interaction integral according to stationary phase method come from points $\boldsymbol{k}_{\otimes}$ in $\Gamma_{\otimes}$ at which the tangential derivative of the phase vanishes.

periodic media (see [11, 62] (section 6.7)) yielding the well known expression for the group velocity of a wavepacket based on the eigenmode $(\bar{n}, \boldsymbol{k})$:

$$\boldsymbol{v}_{\mathrm{gr}}(\bar{n}, \boldsymbol{k}) = \nabla\omega_{\bar{n}}(\boldsymbol{k}). \tag{88}$$

The derivation of (88) is instructive and is given as follows. A wavepacket $\boldsymbol{U}_{\bar{n},\boldsymbol{k}}(\boldsymbol{r}, t)$ based on the Bloch eigenmode $\boldsymbol{G}_{\bar{n}}(\boldsymbol{r}, \boldsymbol{k})$ in d-dimensional periodic medium can be written as

$$\boldsymbol{U}_{\bar{n},\boldsymbol{k}}(\boldsymbol{r}, t) = \frac{1}{(2\pi)^d}\int_{|\tilde{\boldsymbol{k}}-\boldsymbol{k}|\leqslant\delta} \tilde{U}_{\bar{n}}(\tilde{\boldsymbol{k}})\boldsymbol{G}_{\bar{n}}(\boldsymbol{r}, \tilde{\boldsymbol{k}})\mathrm{e}^{-\mathrm{i}\omega_{\bar{n}}(\tilde{\boldsymbol{k}})t}\,\mathrm{d}\tilde{\boldsymbol{k}} \tag{89}$$

where δ is an appropriately small number. Using the property (41) of the Bloch mode $\boldsymbol{G}_{\bar{n}}(\boldsymbol{r}, \boldsymbol{k})$ we get

$$\boldsymbol{U}_{\bar{n},\boldsymbol{k}}(\boldsymbol{r}+\boldsymbol{m}, t) = \frac{1}{(2\pi)^d}\int_{|\tilde{\boldsymbol{k}}-\boldsymbol{k}|\leqslant\delta} \tilde{U}_{\bar{n}}(\tilde{\boldsymbol{k}})\boldsymbol{G}_{\bar{n}}(\boldsymbol{r}, \tilde{\boldsymbol{k}})\mathrm{e}^{\mathrm{i}[(\boldsymbol{m}\cdot\tilde{\boldsymbol{k}})-\omega_n(\tilde{\boldsymbol{k}})t]}\,\mathrm{d}\tilde{\boldsymbol{k}} \tag{90}$$

for any integer valued $\boldsymbol{m}$. Being interested in the wavepacket evolution for large times t and large distances proportional to t, we neglect the fact that $\boldsymbol{m}$ is integer valued and rewrite (90) substituting $\boldsymbol{r} = \boldsymbol{0}$ and $\boldsymbol{m} = \boldsymbol{r}'$ as follows:

$$\boldsymbol{U}_{\bar{n},\boldsymbol{k}}(\boldsymbol{r}', t) \cong \frac{1}{(2\pi)^d}\int_{|\tilde{\boldsymbol{k}}-\boldsymbol{k}|\leqslant\delta} \tilde{U}_{\bar{n}}(\tilde{\boldsymbol{k}})\boldsymbol{G}_{\bar{n}}(\boldsymbol{0}, \tilde{\boldsymbol{k}})\mathrm{e}^{\mathrm{i}[(\boldsymbol{r}'\cdot\tilde{\boldsymbol{k}})-\omega_n(\tilde{\boldsymbol{k}})t]}\,\mathrm{d}\tilde{\boldsymbol{k}}. \tag{91}$$

Applying the standard stationary phase method to the integral in (91) we find that the amplitude of the wavepacket $\boldsymbol{U}_{\bar{n},\boldsymbol{k}}(\boldsymbol{r}',t)$ is not very small only if

$$\nabla_{\boldsymbol{k}}[(\boldsymbol{r}'\cdot\boldsymbol{k})-\omega_n(\boldsymbol{k})t]=\boldsymbol{0} \tag{92}$$

or, equivalently,

$$\boldsymbol{r}'=\nabla_{\boldsymbol{k}}\omega_n(\boldsymbol{k})t. \tag{93}$$

For a typical mode $(\bar{n},\boldsymbol{k})$ and $t=\tau/\varrho$ the amplitude $\boldsymbol{U}_{\bar{n},\boldsymbol{k}}(\boldsymbol{r}',t)$ is proportional to $\varrho^{\frac{d}{2}}$ as $\varrho\to0$, and the wavepacket is spatially localized about the point $\nabla_{\boldsymbol{k}}\omega_n(\boldsymbol{k})t$, indicating that the group velocity $\boldsymbol{v}_{\mathrm{gr}}(\bar{n},\boldsymbol{k})$ is $\nabla_{\boldsymbol{k}}\omega_n(\boldsymbol{k})$ as stated in (88). We would like to remark that here the group velocity describes the wavepacket motion over distances substantially larger than the size of the periodic cell.

Turning now to the first nonlinear response, we deduce from (29), (53), (54) that for $\varrho\to0$

$$\boldsymbol{V}^{(1)}_{\bar{n},\boldsymbol{k}}(\boldsymbol{r},t)\cong\frac{1}{(2\pi)^d}\int_{|\tilde{\boldsymbol{k}}-\boldsymbol{k}|\leqslant\delta}\tilde{V}^{(1)}_{\bar{n}}(\tilde{\boldsymbol{k}},\tau)\boldsymbol{G}_{\bar{n}}(\boldsymbol{r},\tilde{\boldsymbol{k}})\mathrm{e}^{\mathrm{i}[\phi_{\bar{n}}(\tilde{\boldsymbol{k}},\boldsymbol{k}')-\omega_n(\tilde{\boldsymbol{k}})]\tau/\varrho}\,\mathrm{d}\tilde{\boldsymbol{k}}. \tag{94}$$

Taking into account (52) we recast (94) as follows:

$$\boldsymbol{V}^{(1)}_{\bar{n},\boldsymbol{k}}(\boldsymbol{r},t)\cong\frac{1}{(2\pi)^d}\int_{|\tilde{\boldsymbol{k}}-\boldsymbol{k}|\leqslant\delta}\tilde{V}^{(1)}_{\bar{n}}(\tilde{\boldsymbol{k}},\tau)\boldsymbol{G}_{\bar{n}}(\boldsymbol{r},\tilde{\boldsymbol{k}})\mathrm{e}^{-\mathrm{i}[\omega_{\bar{n}'}(\boldsymbol{k}')+\omega_{\bar{n}''}(\tilde{\boldsymbol{k}}-\boldsymbol{k}')]\tau/\varrho}\,\mathrm{d}\tilde{\boldsymbol{k}}. \tag{95}$$

Applying now the argument used for the wavepacket $\boldsymbol{U}_{\bar{n},\boldsymbol{k}}(\boldsymbol{r},t)$ we derive from (95) the following representation for the group velocity of the first nonlinear response:

$$\boldsymbol{v}_{\mathrm{gr}}(\boldsymbol{V}^{(1)}_{\bar{n},\boldsymbol{k}})=\nabla_{\boldsymbol{k}}\omega_{\bar{n}''}(\boldsymbol{k}-\boldsymbol{k}'). \tag{96}$$

In particular, if the GVC (59) is satisfied, then the group velocity of the first nonlinear response, as a wave on its own, matches both group velocities of the interacting modes justifying the equality (60). Observe also that the group velocity $\nabla_{\boldsymbol{k}}\omega_{\bar{n}''}(\boldsymbol{k}-\boldsymbol{k}')$ of the first nonlinear response related to the $(\bar{n},\boldsymbol{k})$-mode evidently differs from the group velocity $\nabla\omega_{\bar{n}}(\boldsymbol{k})$ of the $(\bar{n},\boldsymbol{k})$-mode as a linear wave.

5.2. The group velocity at band-crossing points

In this section we show that the group velocity condition still holds at BC points if the group velocity being the gradient of the phase is interpreted as a multivalued quantity as described in sections 4.1, 4.2.

Let us evaluate the nonlinear interaction integrals at BC points. We carry out the evaluation of the interaction integrals for the space dimension $d=2$. The three-dimensional case $d=3$ is reduced to $d=2$ as it is explained in section 4.2. For simplicity we consider only non-degenerate BC points $\boldsymbol{k}'_{\otimes}$. To find the asymptotic approximation to the interaction integral $I_\delta(\boldsymbol{k}_{\otimes})$ defined by (79) we use the relations (76)–(86). The asymptotic analysis can be ultimately reduced to the analysis of an integral of the following form:

$$I(\varrho)=\int_0^{2\pi}\mathrm{d}\theta\int_0^{\delta}\mathrm{e}^{\mathrm{i}\varphi(r,\theta)\tau/\varrho}Q(r,\theta)r\,\mathrm{d}r,\qquad 0\leqslant\theta\leqslant2\pi, \tag{97}$$

where

$$\varphi(\boldsymbol{k})=\varphi(r,\theta)=\varphi(\boldsymbol{k}_{\otimes})+v_1(k_1-k_{\otimes1})+v_2(k_2-k_{\otimes2})+r\cos(\theta_0)+\mathrm{O}(r^2), \tag{98}$$

$$v_1=\partial_{k_1}\psi(\boldsymbol{k}_{\otimes}),\qquad v_2=\partial_{k_2}\psi(\boldsymbol{k}_{\otimes}) \tag{99}$$

or, in view of (75),

$$\varphi(r,\theta)=\varphi(\boldsymbol{k}_{\otimes})+r[v_1a_1\cos(\theta-\theta_0)+v_2a_2\sin\theta+\cos(\theta_0)]+\mathrm{O}(r^2). \tag{100}$$

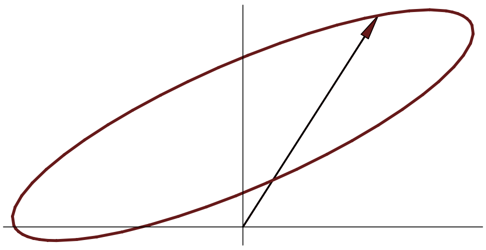

Figure 7. This figure illustrates the GVC held at a BC point $\boldsymbol{k}'_\otimes$ of the phase $\phi_{\vec{n}}(\boldsymbol{k}, \boldsymbol{k}')$ attributed to $\omega_{\vec{n}'}(\boldsymbol{k}')$. The arrow indicates the group velocity $\nabla\omega_{\vec{n}''}(\boldsymbol{k} - \boldsymbol{k}'_\otimes)$, and the elliptic curve is the set of all the values of the group velocity at the BC point $\boldsymbol{k}'_\otimes$ of $\omega_{\vec{n}'}(\boldsymbol{k}')$. The GVC is signified by the tip of the arrow being exactly in the curve, indicating matching of the group velocity $\nabla\omega_{\vec{n}''}(\boldsymbol{k} - \boldsymbol{k}'_\otimes)$ with one of the values of the group velocity $\nabla\omega_{\vec{n}'}(\boldsymbol{k}'_\otimes)$.

The asymptotic analysis of the integral $I(\varrho)$ from (97), based on the stationary phase method, shows that $I(\varrho) \sim \varrho^{q_0}$ for $\varrho \to 0$, where the positive index q_0 attains its smallest value if there exists θ such that

$$\partial_r\varphi(0,\theta) = 0, \qquad \partial_\theta\partial_r\varphi(0,\theta) = 0. \tag{101}$$

Note, that for the phase defined by (100) the conditions (101) determining the points of the dominant contribution to the integral $I(\varrho)$ differ from standard stationary phase conditions

$$\partial_r\varphi = 0, \qquad \partial_\theta\varphi = 0. \tag{102}$$

Substituting (100) into (101) we get

$$v_1 a_1 \cos(\theta - \theta_0) + v_2 a_2 \sin(\theta) + \cos(\theta_0) = 0 \tag{103}$$

$$-v_1 a_1 \sin(\theta - \theta_0) + v_2 a_2 \cos(\theta) = 0. \tag{104}$$

Solving (103) for v_1 and v_2 we find that (103) is equivalent to

$$v_1 = -\frac{\cos(\theta)}{a_1}, \qquad v_2 = -\frac{\sin(\theta - \theta_0)}{a_2}. \tag{105}$$

Observe now that in view of (99) and (86) the equations (105), in turn, are equivalent to

$$\nabla_{\boldsymbol{k}}\varphi(\boldsymbol{k}_\otimes, \theta) = 0. \tag{106}$$

In the case when (105) and, hence, (106) are satisfied we have

$$I(\varrho) \sim \varrho^{5/4}, \qquad \varrho \to 0, \tag{107}$$

whereas if (106) does not hold then

$$I(\varrho) \sim \varrho^2, \qquad \varrho \to 0. \tag{108}$$

Consider now our phase

$$\phi_{\vec{n}}(\boldsymbol{k}, \boldsymbol{k}') = \omega_{\vec{n}}(\boldsymbol{k}) - \omega_{\vec{n}'}(\boldsymbol{k}') - \omega_{\vec{n}''}(\boldsymbol{k} - \boldsymbol{k}') \tag{109}$$

when either $\boldsymbol{k}' = \boldsymbol{k}'_\otimes$ is a BC point for $\omega_{\vec{n}'}(\boldsymbol{k}')$ or $\boldsymbol{k} - \boldsymbol{k}'_\otimes$ is a BC point for $\omega_{\vec{n}''}(\boldsymbol{k} - \boldsymbol{k}')$. Consequently, $\boldsymbol{k}'_\otimes$ is a BC point for the phase $\phi_{\vec{n}}(\boldsymbol{k}, \boldsymbol{k}')$ as a function of $\boldsymbol{k}'$. The condition (106) for the phase $\phi_{\vec{n}}(\boldsymbol{k}, \boldsymbol{k}')$ then turns into the GVC. Namely, it has the same form as in (58) and (59), i.e.

$$\nabla\omega_{\vec{n}'}(\boldsymbol{k}'_\otimes) = \nabla\omega_{\vec{n}''}(\boldsymbol{k} - \boldsymbol{k}'_\otimes) \tag{110}$$

with the multiple valued gradient interpreted as in sections 4.1, 4.2. Figure 7 illustrates the GVC for $d = 2$.

6. The second-harmonic generation

The SHG in photonic crystals has been the subject of both theoretical and experimental studies [23, 41, 48, 49, 58]. In particular, SHG has been achieved experimentally:

(i) at the edges of photonic bands of one-dimensional semiconductor photonic crystals [23];
(ii) in a three-dimensional photonic crystal structure [41];
(iii) in one-dimensional periodic photonic crystal with a defect [58];
(iv) in a double resonator semiconductor microcavity [49].

Numerical studies carried out in [48] suggest a significant enhancement of SHG near photonic band edges. The enhancement stems from the low group velocity near band edges. Low or even zero group velocity can also occur in nonreciprocal magnetic photonic crystals in the frozen mode regime [31], that may be an alternative to the band-edge mechanism.

The SHG can be considered as a mode interaction process within our approach subject to the limitations described in sections 1.2 and 3.1. This can be performed as follows. Consider the nonlinear interaction between a mode $(\bar{n}', \boldsymbol{k}')$ with itself and its impact on a mode $(\bar{n}, \boldsymbol{k})$. We can look at that as there are two modes $(\bar{n}', \boldsymbol{k}')$ and $(\bar{n}'', \boldsymbol{k}'')$ such that

$$\bar{n}' = \bar{n}'', \qquad \boldsymbol{k}' = \boldsymbol{k}'' \bmod(2\pi). \tag{111}$$

Hence, in view of the phase matching condition $\boldsymbol{k}'' = \boldsymbol{k} - \boldsymbol{k}'$, we must set

$$\boldsymbol{k}' = \boldsymbol{k}'' = \boldsymbol{k}/2 \bmod(2\pi). \tag{112}$$

The above implies that the mode $(\bar{n}', \boldsymbol{k}/2)$ interacting with itself impacts the mode $(\bar{n}, \boldsymbol{k})$. Observe now that, in view of (111) and (112), the mode $(\bar{n}', \boldsymbol{k}/2)$ self-interaction always satisfies the GVC (59) indicating a stronger nonlinear interaction. As to the FMC (57), it requires

$$\omega_{\bar{n}}(\boldsymbol{k}) = 2\omega_{\bar{n}'}(\boldsymbol{k}/2). \tag{113}$$

In other words, if there exists $\boldsymbol{k}$ satisfying (113), then there will be a strong nonlinear self-interaction of the mode $(\bar{n}', \boldsymbol{k}/2)$ with an impact on the mode $(\bar{n}, \boldsymbol{k})$ of the exactly two times higher frequency.

The nonlinear interaction indices related to the SHG are listed in tables 3–8. They indicate, in particular, that the SHG is one of the strongest nonlinear interactions, and often just the strongest. The reason for this is the invariance of the phase with respect to the transformation $\boldsymbol{k}' \leftrightarrow \boldsymbol{k} - \boldsymbol{k}'$. Evidently $\boldsymbol{k}' = \boldsymbol{k}/2$ is the fixed point of the transformation.

As already pointed out in section 1.2, the SHG when both the fundamental and the second-harmonic frequencies tuned to photonic band edges [23, 48], can be within the limits of the above approach.

7. Classification of nonlinear interactions

The nonlinear interactions can be studied and classified based on the first nonlinear response $\tilde{V}_{\bar{n}}^{(1)}(\boldsymbol{k}, \tau)$ to different wavepackets as they become almost monochromatic, i.e. $\varrho \to 0$. The classification is based on interaction indices and proceeds as follows.

To evaluate the impact of a pair of modes $(\bar{n}', \boldsymbol{k}')$ and $(\bar{n}'', \boldsymbol{k}'')$, with $\boldsymbol{k}'' = \boldsymbol{k} - \boldsymbol{k}'$, on the mode $(\bar{n}, \boldsymbol{k})$ we apply the standard stationary phase approach. Namely, we use the excitation current $\boldsymbol{J}(\boldsymbol{r}, t)$ in the form of a wavepacket composed of modes from a small vicinity of the chosen modes $(\vec{n}', \boldsymbol{k}')$ and $(\vec{n}'', \boldsymbol{k}'')$. This excitation current, in view of (48) and (50), can be written as follows:

$$\boldsymbol{J}(\boldsymbol{r}, t) = \frac{\varrho}{(2\pi)^3} \int_{B_\delta(\boldsymbol{k}', \boldsymbol{k}'')} \tilde{j}_n(\boldsymbol{m}, \tau) \boldsymbol{G}_{\vec{n}}(\boldsymbol{r}, \boldsymbol{m}) \mathrm{e}^{-\mathrm{i}\omega_{\vec{n}}(\boldsymbol{m})\tau/\varrho} \, \mathrm{d}\boldsymbol{m}, \tag{114}$$

$$B_\delta(\boldsymbol{k}', \boldsymbol{k}'') = \{|\boldsymbol{m} - \boldsymbol{k}'| \leqslant \delta\} \cup \{|\boldsymbol{m} - \boldsymbol{k}''| \leqslant \delta\} \tag{115}$$

$$\tilde{j}_n(\boldsymbol{m}, \tau) = 0 \qquad \text{if } \boldsymbol{m} \text{ is not in } B_\delta(\boldsymbol{k}', \boldsymbol{k}'') \tag{116}$$

with a fixed small δ. The corresponding linear response is

$$\tilde{V}_{\vec{n}}^{(0)}(\boldsymbol{k}, \tau) = -\int_0^\tau \tilde{j}_{\vec{n}}(\boldsymbol{k}, \tau_1) \, \mathrm{d}\tau_1; \qquad \tilde{V}_{\vec{n}}^{(0)}(\boldsymbol{k}, \tau) = 0 \qquad \text{if } \boldsymbol{k} \text{ is not in } B_\delta(\boldsymbol{k}', \boldsymbol{k}''). \tag{117}$$

We also assume $\tilde{j}_n(\boldsymbol{k}, \tau)$, and consequently $\tilde{V}_{\vec{n}}^{(0)}(\boldsymbol{k}, \tau)$, to be smooth functions of $\boldsymbol{k}$.

Now, keeping in mind (53) and (54), we introduce in the consideration the following interaction integral:

$$\mathcal{I}_\delta(\vec{n}, \boldsymbol{k}, \boldsymbol{k}', \tau) = \int_0^\tau \mathrm{d}\tau_1 \int_{B_\delta(\boldsymbol{k}', \boldsymbol{k}'')} \mathrm{e}^{\mathrm{i}\phi_{\vec{n}}(\boldsymbol{k}, \boldsymbol{m})\tau_1/\varrho} \, \tilde{Q}_{\vec{n}}[\tilde{V}^{(0)} | \, \boldsymbol{k}, \boldsymbol{m}, \tau_1] \, \mathrm{d}\boldsymbol{m} \tag{118}$$

resulting in the first nonlinear response

$$\tilde{V}_{\vec{n}}^{(1)}(\boldsymbol{k}, \tau) = \frac{\alpha}{\varrho} \mathcal{I}_\delta(\vec{n}, \boldsymbol{k}, \boldsymbol{k}', \tau). \tag{119}$$

Thus, the interaction integral $\mathcal{I}_\delta(\vec{n}, \boldsymbol{k}, \boldsymbol{k}', \tau)$ defined by (118) accounts for the nonlinear impact of the modes $(\vec{n}', \boldsymbol{k}')$ and $(\vec{n}'', \boldsymbol{k}'')$, with $\boldsymbol{k}'' = \boldsymbol{k} - \boldsymbol{k}'$, on the mode $(\vec{n}, \boldsymbol{k})$. It plays a key role in the analysis and classification of nonlinear interactions in periodic dielectric media. As to the asymptotic approximation of $\mathcal{I}_\delta(\vec{n}, \boldsymbol{k}, \boldsymbol{k}', \tau)$ as $\varrho \to 0$, it is based, in particular, on the stationary phase method [7, 26, 28, 29, 32, 51], applied to the phase $\phi_{\vec{n}}(\boldsymbol{k}, \boldsymbol{m})$ as a function of $\boldsymbol{m}$ in an infinitesimally small vicinity of $\boldsymbol{k}'$. Ultimately, it is reduced to the study of two cases:

(i) noncritical points for which the integral decays faster than any power ϱ;
(ii) *critical points: simple and band-crossing ones.*

The *simple critical points* $\boldsymbol{k}'_*$ are defined as points for which the gradient of the phase $\nabla_{\boldsymbol{m}}\phi_{\vec{n}}(\boldsymbol{k}, \boldsymbol{k}'_*)$, being well defined, vanishes. For the phase (52) this condition is reduced to the GVC, (58), (59), where $\boldsymbol{k}'_*$ is such that both eigenfrequencies $\omega_{\vec{n}'}(\boldsymbol{k}'_*)$ and $\omega_{\vec{n}''}(\boldsymbol{k} - \boldsymbol{k}'_*)$ are simple, i.e. of the multiplicity one, and, consequently, the phase $\phi_{\vec{n}}(\boldsymbol{k}, \boldsymbol{m})$ is smooth in $\boldsymbol{m}$ at $\boldsymbol{m} = \boldsymbol{k}'_*$.

The second type of critical points are BC points where either $\omega_{\vec{n}'}(\boldsymbol{k}')$ or $\omega_{\vec{n}''}(\boldsymbol{k} - \boldsymbol{k}')$ is not differentiable. Such points $\boldsymbol{k}'_\otimes$ arise when $\omega_{\vec{n}'}(\boldsymbol{k}'_\otimes)$ is the eigenfrequency of the multiplicity 2 or higher, that that the case when a two or bands have a common point. A generic BC point is of multiplicity 2. The BC points satisfy the GVC for multiple valued gradients as described in sections 4.1, 4.2 (see formula (86)). We will refer to those points as satisfying the GVC(BC) condition. Therefore, every critical point must satisfy either the GVC or GVC(BC) conditions.

We classify nonlinear interactions based on their strength measured by the asymptotic behaviour as $\varrho \to 0$ of the related interaction integrals. It follows from the stationary phase method that if the group velocity condition (simple or generalized for BC points) is not satisfied, then the interaction integral $\mathcal{I}_\delta(\vec{n}, \boldsymbol{k}, \boldsymbol{k}', \tau)$ decays faster than any positive power of ϱ as $\varrho \to 0$ [12]. In contrast, if the group velocity condition is satisfied (simple or generalized for BC points), the interaction integral $\mathcal{I}_\delta(\vec{n}, \boldsymbol{k}, \boldsymbol{k}', \tau)$ will be of order ϱ^{q_0} where $1/2 \leqslant q_0 \leqslant 5/2$ (see table 2).

As explained previously *the GVC (simple or generalized for BC points) must be satisfied for stronger nonlinear interactions. For this reason, from now on all strong interactions*

Table 1. Abbreviations for the classes of nonlinear interactions. GV stands for the group velocity, and BC stands for band crossing. Every table entry indicates that the conditions in the corresponding row and the column are satisfied. The entry itself is an abbreviation used to refer to the related properties.

	Simple GVC holds	GVC(BC) holds
FMC holds: cumulative response	CGV	CBC
FMC does not hold: instantaneous response	IGV	IBC

Table 2. Interaction indices of the critical points for the quadratic nonlinearity. The fractions in the entries indicate the permitted values of the index q_0. Since the interaction integral is of the order ρ^{q_0} as $\rho \to 0$ the smaller values of q_0 correspond to stronger nonlinear interactions. The largest values of q_0 correspond to nondegenerate simple critical points with $q_{\mathcal{T}} = d/2$. Higher degeneracy yields smaller q_0 and, hence, stronger nonlinear interactions.

q_0	Cumulative CGV $q_0 = q_{\mathcal{T}}$	Instantaneous IGV $q_0 = q_{\mathcal{T}} + 1$	Cumulative CBC $q_0 = q_{\mathcal{T}\otimes}$
$d = 1$	$\frac{1}{2}$	$\frac{5}{4}$; $\frac{4}{3}$; $\frac{3}{2}$	None
$d = 2$	$\frac{3}{4}$; $\frac{5}{6}$; 1	$\frac{5}{3}$; $\frac{7}{4}$; $\frac{11}{6}$; 2	$\frac{5}{4}$; 2
$d = 3$	$\frac{7}{6}$; $\frac{5}{4}$; $\frac{4}{3}$; $\frac{3}{2}$	2; $\frac{17}{8}$; $\frac{13}{6}$; $\frac{11}{5}$; $\frac{9}{4}$; $\frac{7}{3}$; $\frac{5}{2}$	$\frac{3}{2}$; $\frac{7}{4}$; $\frac{9}{4}$; $\frac{7}{3}$; $\frac{5}{2}$

are assumed to satisfy it. Then the most basic classification is based on the fulfilment of the FMC condition. This classification is summarized in the table 1. There are three classes of interactions which may account for leading contributions: CGV, CBC and IGV. The interactions of the IBC class are always subordinate.

Note that the selection rules involve only the Bloch dispersion relations since the susceptibility tensors were assumed to be periodic of the same common period. If the periods of the susceptibility tensors do not match, the selection rules have to be slightly modified by appropriate shifts (depending on the mismatch of the periods) of the quasimomenta in the dispersion functions. Namely, the phase matching condition $\boldsymbol{k} = \boldsymbol{k}' + \boldsymbol{k}''(\mathrm{mod}\, 2\pi)$ is replaced by $\boldsymbol{k} \pm \boldsymbol{g} = \boldsymbol{k}' + \boldsymbol{k}''(\mathrm{mod}\, 2\pi)$ if the nonlinearity is spatially modulated by $\sin(\boldsymbol{g} \cdot \boldsymbol{r})$. Note that the corresponding modification of the phase $\phi_{\vec{n}}(\boldsymbol{k}, \boldsymbol{k}')$ from (109) to

$$\phi_{\vec{n}}(\boldsymbol{k}, \boldsymbol{k}') = \omega_{\vec{n}}(\boldsymbol{k}) - \omega_{\vec{n}'}(\boldsymbol{k}') - \omega_{\vec{n}''}(\boldsymbol{k} - \boldsymbol{k}' \pm \boldsymbol{g}) \tag{120}$$

clearly preserves the form of the GVC. This natural extension of the formalism accounts for the so-called quasi-phase-matching method commonly used to enhance nonlinear interaction through the FMC, see, for instance [30] and references therein.

A finer classification of nonlinear interaction is based on the index of interaction $q_0(\boldsymbol{k})$. The possible values of the interaction index for all space dimensions $d = 1$, 2 and 3 are collected in table 2.

Every entry in table 2 contains several values of q_0. Since the interaction integral is of the order ϱ^{q_0} as $\varrho \to 0$, the smaller values of q_0 correspond to stronger nonlinear interactions. The largest values of q_0 for simple points correspond to non-degenerate simple critical points with $q_{\mathcal{T}} = \frac{d}{2}$. Higher degeneracy yields smaller q_0 and, hence, stronger nonlinear interactions. Note that for the homogeneous dispersionless medium the index $q_0 = \frac{d-1}{2}$ is smaller than all the presented values in table 2 [12]. This can be explained by the higher symmetry of a homogeneous dispersionless medium, and, consequently, higher degeneracy of critical points

Table 3. Spatial dimension $d = 1$, FMC is satisfied, $D_{\mathcal{M}} \leqslant 2$.

ϱ^{q_0}	Phase canonical form	$D_{\mathcal{M}}$	$H_{\mathcal{M}}$	Extra selection rules
$\varrho^{1/2}$	$\pm\tilde{k}_1^2, \quad A_1$	0	1	non-deg.
$\varrho^{1/2}$	$\pm\tilde{k}_1^2, \quad A_1$	0	1	SHG

Table 4. Spatial dimension $d = 2$, FMC is satisfied, $D_{\mathcal{M}} \leqslant 4$.

ϱ^{q_0}	Phase canonical form	$D_{\mathcal{M}}$	$H_{\mathcal{M}}$	Extra selection rules
ϱ^{1}	$\pm\tilde{k}_1^2 \pm \tilde{k}_2^2, \quad A_1^2$	1	2	non-deg.
$\varrho^{5/6}$	$\pm\tilde{k}_1^2 \pm \tilde{k}_2^3, \quad A_1 \times A_2$	0	1	deg.
ϱ^{1}	$\pm\tilde{k}_1^2 \pm \tilde{k}_2^2, \quad A_1^2$	1	2	SHG
$\varrho^{3/4}$	$\pm\tilde{k}_1^2 \pm \tilde{k}_2^4, \quad A_1 \times A_3$	0	1	SHG-deg.

Table 5. Spatial dimension $d = 3$, FMC is satisfied, $D_{\mathcal{M}} \leqslant 6$.

ϱ^{q_0}	Phase canonical form	$D_{\mathcal{M}}$	$H_{\mathcal{M}}$	Extra selection rules
$\varrho^{3/2}$	$\pm\tilde{k}_1^2 \pm \tilde{k}_2^2 \pm \tilde{k}_3^2, \quad A_1^3$	2	3	non-deg.
$\varrho^{8/6}$	$\pm\tilde{k}_1^2 \pm \tilde{k}_2^2 \pm \tilde{k}_3^3, \quad A_1^2 \times A_2$	1	2	deg.
$\varrho^{7/6}$	$\pm\tilde{k}_1^2 \pm \tilde{k}_2^2 \pm \tilde{k}_3^4, \quad A_1^2 \times A_3$	0	2	deg.[2]
$\varrho^{3/2}$	$\pm\tilde{k}_1^2 \pm \tilde{k}_2^2 \pm \tilde{k}_3^2, \quad A_1^3$	2	3	SHG
$\varrho^{5/4}$	$\pm\tilde{k}_1^2 \pm \tilde{k}_2^2 \pm \tilde{k}_3^4, \quad A_1^2 \times A_3$	1	2	SHG-deg.
$\varrho^{7/6}$	$\pm\tilde{k}_1^2 \pm \tilde{k}_2^2 \pm \tilde{k}_3^6, \quad A_1^2 \times A_5$	0	2	SHG-deg.[2]

Table 6. Spatial dimension $d = 1$, FMC is not satisfied, $D_{\mathcal{M}} \leqslant 2$.

ϱ^{q_0}	Phase canonical form	$D_{\mathcal{M}}$	$H_{\mathcal{M}}$	Extra selection rules
$\varrho^{3/2}$	$\pm\tilde{k}_1^2, \quad A_1$	1	1	non-deg.
$\varrho^{4/3}$	$\pm\tilde{k}_1^3, \quad A_2$	0	0	deg.
$\varrho^{3/2}$	$\pm\tilde{k}_1^2, \quad A_1$	1	1	SHG
$\varrho^{5/4}$	$\pm\tilde{k}_1^4, \quad A_3$	0	0	SHG-deg.

compared to a periodic medium. One can also see from the table that instantaneous interactions for which the FMC does not hold, are weaker than the simple cumulative interaction.

7.1. Finer classification of nonlinear interactions

It follows from the previous sections that for a quadratic nonlinearity triads of modes can interact or, in other words, two modes make an impact on the third one. Those modes are parametrized by three band indices $\vec{n} = (\bar{n}, \bar{n}', \bar{n}'')$ and two quasimomenta $\boldsymbol{k}$ and $\boldsymbol{k}'$, since the third one $\boldsymbol{k}'' = \boldsymbol{k} - \boldsymbol{k}'$. The intensity of the mode interaction is ultimately determined by the asymptotic behaviour of an oscillatory integral of the form

$$I_\delta(\tau) = \int_0^\tau \mathrm{d}\tau_1 \int_{|\tilde{\boldsymbol{k}}-\boldsymbol{k}'|\leqslant\delta} \mathrm{e}^{\mathrm{i}\phi_{\vec{n}}(\boldsymbol{k},\tilde{\boldsymbol{k}})\tau_1/\varrho} A(\tilde{\boldsymbol{k}}, \tau_1)\,\mathrm{d}\tilde{\boldsymbol{k}} \sim \varrho^{q_0}, \qquad \varrho \to 0, \quad (121)$$

Table 7. Spatial dimension $d = 2$, FMC is not satisfied, $D_{\mathcal{M}} \leqslant 4$.

ϱ^{q_0}	Phase canonical form	$D_{\mathcal{M}}$	$H_{\mathcal{M}}$	Extra selection rules
ϱ^{2}	$\pm\tilde{k}_1^2 \pm \tilde{k}_2^2, \quad A_1^2$	2	2	non-deg.
$\varrho^{11/6}$	$\pm\tilde{k}_1^2 \pm \tilde{k}_2^3, \quad A_1 \times A_2$	1	1	deg.
$\varrho^{7/4}$	$\pm\tilde{k}_1^2 \pm \tilde{k}_2^4, \quad A_1 \times A_3$	0	1	deg.^{2}
ϱ^{2}	$\pm\tilde{k}_1^2 \pm \tilde{k}_2^2, \quad A_1^2$	2	2	SHG
$\varrho^{7/4}$	$\pm\tilde{k}_1^2 \pm \tilde{k}_2^4, \quad A_1 \times A_3$	1	1	SHG-deg.
$\varrho^{5/3}$	$\pm\tilde{k}_1^2 \pm \tilde{k}_2^6, \quad A_1 \times A_5$	0	1	SHG-deg.^{2}

Table 8. Spatial dimension $d = 3$, FMC is not satisfied, $D_{\mathcal{M}} \leqslant 6$.

ϱ^{q_0}	Phase canonical form	$D_{\mathcal{M}}$	$H_{\mathcal{M}}$	Extra selection rules
$\varrho^{5/2}$	$\pm\tilde{k}_1^2 \pm \tilde{k}_2^2 \pm \tilde{k}_3^2, \quad A_1^3$	3	3	non-deg.
$\varrho^{7/3}$	$\pm\tilde{k}_1^2 \pm \tilde{k}_2^2 \pm \tilde{k}_3^3, \quad A_1^2 \times A_2$	2	2	deg.
$\varrho^{9/4}$	$\pm\tilde{k}_1^2 \pm \tilde{k}_2^2 \pm \tilde{k}_3^4, \quad A_1^2 \times A_3$	1	2	deg.^{2}
$\varrho^{11/5}$	$\pm\tilde{k}_1^2 \pm \tilde{k}_2^2 \pm \tilde{k}_3^5, \quad A_1^2 \times A_4$	0	2	deg.^{3}
$\varrho^{13/6}$	$\pm\tilde{k}_1^2 \pm \tilde{k}_2^3 \pm \tilde{k}_2\tilde{k}_3^2, \quad A_1 \times D_4$	0	1	deg.^{3} + $\{H_{\mathcal{M}} = 1\}$
$\varrho^{5/2}$	$\pm\tilde{k}_1^2 \pm \tilde{k}_2^2 \pm \tilde{k}_3^2, \quad A_1^3$	3	3	SHG.
$\varrho^{5/4}$	$\pm\tilde{k}_1^2 \pm \tilde{k}_2^2 \pm \tilde{k}_3^4, \quad A_1^2 \times A_3$	2	2	SHG-deg.
$\varrho^{13/6}$	$\pm\tilde{k}_1^2 \pm \tilde{k}_2^2 \pm \tilde{k}_3^6, \quad A_1^2 \times A_5$	1	2	SHG-deg.^{2}
$\varrho^{17/8}$	$\pm\tilde{k}_1^2 \pm \tilde{k}_2^2 \pm \tilde{k}_3^8, \quad A_1^2 \times A_7$	0	2	SHG-deg.^{3}
ϱ^{2}	$\pm\tilde{k}_1^2$ + 4th order	0	1	SHG-deg.^{3} + $\{H_{\mathcal{M}} = 1\}$

with $\delta \ll 1$ and the phase

$$\phi_{\bar{n}}(\boldsymbol{k}, \tilde{\boldsymbol{k}}) = \omega_{\bar{n}}(\boldsymbol{k}) - \omega_{\bar{n}'}(\tilde{\boldsymbol{k}}) - \omega_{\bar{n}''}(\boldsymbol{k} - \tilde{\boldsymbol{k}}). \tag{122}$$

According to the theory of oscillatory integrals in a typical situation the asymptotic approximation to $I_\delta(\tau)$ defined by (121) is determined by the leading terms in the Taylor series expansion of $\phi_{\bar{n}}(\boldsymbol{k}, \tilde{\boldsymbol{k}})$ at the point $\boldsymbol{k}'$. Hence, those leading terms, or their reduced (by a proper change of variables) canonical polynomial forms, can be used for finer classification of the interaction. We analysed all possibilities for the generic phase $\phi_{\bar{n}}(\boldsymbol{k}, \tilde{\boldsymbol{k}})$ defined by (122) and collected the results in tables 3–8. The phase canonical forms in the tables are given in the related reduced variables.

When classifying nonlinear interactions we consider only robust interactions that persist under small perturbation of dispersion relations $\omega_{\bar{n}}(\boldsymbol{k})$. *It is also assumed that there are no 'hidden symmetries'. In our analysis we assumed no symmetries for* $\omega_{\bar{n}}(\boldsymbol{k})$. *The presence of any symmetry, for instance* $\omega_{\bar{n}}(\boldsymbol{k}) = \omega_{\bar{n}}(-\boldsymbol{k})$, *would require a special analysis and further extension of the tables.*

We will use the following quantities to characterize the nonlinear interactions.

q_0 is *the interaction* index defined for nonlinearly interacting modes. The relevant nonlinear interaction is proportional to ϱ^{q_0} as $\varrho \to 0$ and, hence, the lesser the index q_0 the stronger the nonlinear interaction. For instance, for any interacting modes which do not satisfy the GVC, we have $q_0 = \infty$ that indicates an extremely weak nonlinear interaction. Keeping that in mind, *we always assume that interacting modes satisfy the GVC.*

Table 9. The basic information of the interaction indices q_0 and the dimension $D_{\mathcal{M}}$ of the manifold of interacting modes.

	$D_{\mathcal{M}}$				
Interaction index q_0	0	1	2	3	4
Spatial dimension $d = 1$	—	—	0	—	—
Spatial dimension $d = 2$	—	—	$\frac{1}{3}$	$\frac{1}{2}$	—
Spatial dimension $d = 3$	—	—	$\frac{3}{4}$	$\frac{5}{6}$	1

Table 10. The information on the indices q_0 of the strongest nonlinear interaction for anisotropic dispersionless homogeneous and generic dispersive, in particular periodic, media.

	Medium	
The index q_0 of the strongest interaction ϱ^{q_0}	Ideal homogeneous	Periodic
Spatial dimension $d = 1$	0	$\frac{1}{2}$
Spatial dimension $d = 2$	$\frac{1}{3}$	$\frac{3}{4}$
Spatial dimension $d = 3$	$\frac{3}{4}$	$\frac{7}{6}$

$\mathcal{M}_{\boldsymbol{k},\boldsymbol{k}'}$ is a *manifold of interacting modes* (described for the quadratic nonlinearity by pairs of the quasimomenta $\boldsymbol{k}$, $\boldsymbol{k}'$) selected by certain selection rule/rules.

$D_{\mathcal{M}}$ is the *topological dimension* of $\mathcal{M}_{\boldsymbol{k},\boldsymbol{k}'}$ which naturally does not exceed $2d$. It indicates 'how many' modes are involved in the relevant interactions. The larger $D_{\mathcal{M}}$ the 'more modes' have the particular interaction.

$H_{\mathcal{M}}$ is the *rank of the Hessian with respect to* $\boldsymbol{k}'$ *of the phase* at points in $\mathcal{M}_{\boldsymbol{k},\boldsymbol{k}'}$ which naturally does not exceed d. This indicates the degree of phase degeneration. The smaller the quantity $H_{\mathcal{M}}$, the more modes in the relevant wavepacket will interact constructively resulting in a stronger nonlinear interaction and, hence, in a lesser interaction index q_0. In the tables below we also use the following abbreviations.

GVC stands for the regular group velocity matching condition for a differentiable phase.

GVC(BC) stands for the group velocity matching condition at band-crossing points.

FMC stands for the frequency matching condition.

'SHG' stands for second harmonic generation.

'non-deg.' stands for non-degenerate points in the sense of the stationary phase method.

'deg.' stands for degenerate points in the sense of the stationary phase method.

'deg.^{2}' and 'deg.^{3}' stand for 'double' and 'triple' degenerate points having higher degrees of degeneration compared with the regular degenerate points.

'SHG-deg.', 'SHG-deg.^{2}' and 'SHG-deg.^{3}' stand for the second harmonic generation when the related points are degenerate or degenerate of higher degrees.

A_m, D_m stands for types (classes) of singular points (see [6]).

7.2. *Comparison of nonlinear interaction in dispersionless homogeneous and periodic media*

For an ideal homogeneous dispersionless medium, when $\omega(\boldsymbol{k}) = C|\boldsymbol{k}|$, the GVC coincides with the phase matching condition and, hence, can always be satisfied. For a general anisotropic homogeneous dispersionless medium one can show that FMC can also always be satisfied. Assuming that both GVC and FMC hold we collected in table 9 the basic information for the interaction indices and the dimension $D_{\mathcal{M}}$ of the manifold of interacting modes.

For comparison we collected, in table 10, the information regarding the indices q_0 of the strongest nonlinear interaction for anisotropic dispersionless homogeneous and generic dispersive, in particular periodic, media. One can clearly see from table 10 that the introduction of periodicity weakens the nonlinear interactions under study.

8. Medium dispersion and nonlinear interactions

It is well known that dispersive properties of a medium play an important role in nonlinear wave interaction (for isotropic media see [36] and references therein). For the nonlinear regimes under study the dispersion relations of the underlying linear medium are instrumental for their formation. In particular, as it is shown in [12] and in section 7, the selection of stronger interactions is ultimately based on the dispersion relations. From this perspective, one can view the introduction of a spatial periodicity into the medium as a factor leading to a fundamental change in the dispersion relations, namely formation of spectral bands with corresponding periodic in $\boldsymbol{k}$ dispersion relations $\omega_n(\boldsymbol{k})$.

As explained in the previous section, the introduction of spatial periodicity in an ideal dispersionless homogeneous nonlinear medium would weaken nonlinear interactions. But in the case of a dispersive homogenous medium such a general comparison is hard to make. The origin of the dispersion is not essential for our analysis, and we can certainly state that for a generic homogeneous nonlinear dispersive medium all nonlinear regimes we study are covered by the above tables of indices.

If one has control over some parameters of the periodic medium, for instance, dimensions of the primitive cell, then by making appropriate adjustments one can achieve nonlinear regimes of higher level of nonlinear interactions according to the tables given in the preceding sections. We have to remember though that our comparative analysis of the nonlinear interactions is based on the fundamental assumption that the dispersion relations $\omega_n(\boldsymbol{k})$ are generic and do not have any 'hidden' symmetries unknown to us. If there are any symmetries one would have to carry out an additional analysis. We expect any additional symmetry to produce stronger nonlinear interactions.

Acknowledgment and disclaimer

The efforts of A Babin and A Figotin were sponsored by the Air Force Office of Scientific Research, Air Force Materials Command, USAF, under grant number F49620-01-1-0567. The US Government is authorized to reproduce and distribute reprints for governmental purposes notwithstanding any copyright notation thereon. The views and conclusions contained herein are those of the authors and should not be interpreted as necessarily representing the official policies or endorsements, either expressed or implied, of the Air Force Office of Scientific Research or the US Government.

References

[1] 2000 Optical gap solitons: past, present, and future; theory and experiments *Chaos* **9** 584–9
[2] Agrawal G 1995 *Nonlinear Fiber Optics* (New York: Academic)
[3] Aközbek N and John S 1998 Optical solitary waves in two- and three-dimensional nonlinear photonic band-gap structures *Phys. Rev.* E **57** 2287–319
[4] Atai J and Malomed B A 2000 Bragg-grating solitons in a semilinear dual-core system *Phys. Rev.* E **60** 8713–18
[5] Arnold V I *Methods of Classical Mechanics (Springer Graduate Texts in Mathematics vol 60)* (New York: Springer)

[6] Arnold V I, Gusein-Zade S M and Varchenko A N 1985 *Singularities of Differentiable Mappings (Monographs in Mathematics vol 82)* vol 1 (Basle: Birkhauser)
[7] Arnold V I, Gusein-Zade S M and Varchenko A N 1988 *Singularities of Differentiable Mappings (Monographs in Mathematics vol 83)* vol 2 (Basle: Birkhauser)
[8] Arraf A and de Sterke C M 1998 Coupled-mode equations for quadratically nonlinear deep gratings *Phys. Rev.* E **58** 7951–8
[9] Arraf A, He H and de Sterke C M 1999 Deep gratings with a χ^2 nonlinearity: analysis and solutions *Opt. Fiber Technol.* **5** 223–34
[10] Arraf A, de Sterke C M and He H 2001 Bright stationary solitary waves in deep gratings with a quadratic nonlinearity *Phys. Rev.* E **63** 026611
[11] Ashcroft N and Mermin N 1976 *Solid State Physics* (New York: Holt, Rinehart and Winston)
[12] Babin A and Figotin A 2001 Nonlinear photonic crystals: I. Quadratic nonlinearity *Waves Random Media* **11** R31–102
[13] Belyakov V 1992 *Diffraction Optics of Complex-Structured Periodic Medium* (Berlin: Springer)
[14] Berger V 1998 Nonlinear photonic crystals *Phys. Rev. Lett.* **81** 4136–9
[15] Broderick N G R, Ross G W, Offerhous H L, Richardson D J and Hanna D C 2000 Hexagonally poled lithium niobate: a two-dimensional nonlinear photonic crystal *Phys. Rev. Lett.* **84** 4345–8
[16] Butcher P and Cotter D 1990 *The Elements of Nonlinear Optics* (Cambridge: Cambridge University Press)
[17] Boyd R 1992 *Nonlinear Optics* (New York: Academic)
[18] Centini M, D'Aguanno G, Scalora M, Sibilia C, Bertolotti M, Bloemer M J and Bowden C M 2001 Simultaneously phase-matched enhanced second and third harmonic generation *Phys. Rev.* E **64** 046606
[19] Carrasco S, Torres J P, Artigas D and Torner L 2000 Generation of multicolor spatial solitons with pulsed light *Opt. Commun.* **192** 347–55
[20] Cojocaru C, Martorell J, Vilaseca R, Trull J and Fazio E 1999 Active reflection via a phase-insensitive quadratic nonlinear interaction within a microcavity *Appl. Phys. Lett.* **74** 504–6
[21] Cojocaru C, Vilaseca R, Martorell J, Carvajal J, Massons J and Diaz F 2001 Actively induced transmission via a quadratic nonlinear optical interaction in a potassium titanyl phosphate microcavity *Appl. Phys. Lett.* **79** 4479–81
[22] Conti C, Trillo S and Assanto G 1997 Bloch function approach for parametric gap solitons *Opt. Lett.* **22** 445–7
[23] Dumeige Y, Vidakovic P, Sauvage S, Sagnes I, Levenson J A, Sibilia C, Centini M, D'Aguanno G and Scalora M 2001 Enhancement of second-harmonic generation in a one-dimensional semiconductor photonic band gap *Appl. Phys. Lett.* **78** 3021–3
[24] Eggleton B J, de Sterke C M and Slusher R E 1997 Nonlinear pulse propagation in Bragg gratings *J. Opt. Soc. Am.* B **14** 2980–93
[25] Eggleton B J, Slusher R E, de Sterke C M, Krug P A and Sipe J E 1996 Bragg grating solitons *Phys. Rev. Lett.* **76** 1627–30
[26] Estrada R and Kanwal R 1994 *Asymptotic Analysis: A Distributional Approach* (Basle: Birkhäuser)
[27] Fedorjuk M V 1987 *Asimptotika Integraly i Rjady* (Moscow: Nauka)
[28] Fedorjuk M V 1962 The method of stationary phase for multiple integrals *J. Commun. Math. Math. Phys.* **2** 145–50
[29] Fedorjuk M V 1977 *The Saddle-Point Method* (Moscow: Nauka)
[30] Fejer M M, Magel G A, Jundt D H and Byer R L 1992 Quasi-phase-matched second harmonic generation: tuning and tolerances *IEEE J. Quantum. Electron.* **28** 2631–54
[31] Figotin A and Vitebsky I 2001 Nonreciprocal magnetic photonic crystals *Phys. Rev.* E **63** 1–17
[32] Felsen L and Marcuvits N 1994 *Radiation and Scattering of Waves* (Oxford: Oxford University Press)
[33] Goul'kov M, Odoulov S, Naumova I, Agullo-Lopez F, Calvo G, Podivilov E, Sturman B and Pruneri V 2001 Degenerate parametric light scattering in periodically poled $LiNbO_3$:Y:Fe *Phys. Rev. Lett.* **86** 4021–4
[34] Haus J, Viswanathan, Scalora M, Kalocsai A, Cole J and Theimer J 1998 Enhanced second-harmonic generation in media with a weak periodicity *Phys. Rev.* A **57** 2120–8
[35] He H and Drummond P D 1997 Ideal soliton environment using parametric band gaps *Phys. Rev. Lett.* **78** 4311–15
[36] He H and Drummond P D 1998 Theory of multidimensional parametric band-gap simultons *Phys. Rev.* E **58** 5025–46
[37] Iizuka T and de Sterke C M 2000 Corrections to coupled mode theory for deep gratings *Phys. Rev.* E **61** 4491–9
[38] Kappeler T 1988 Multiplicities of the eigenvalues of the Schrödinger equation in any dimension *J. Funct. Anal.* **77** 346–51
[39] Kato T 1995 *Perturbation Theory for Linear Operators* (Berlin: Springer)

[40] Kumasako J, Matsumoto M and Waiyapot S 2000 Linear stability analysis of dispersion-managed solitons controlled by filters *J. Lightwave Technol.* **18** 1064–8
[41] Martorell J, Vilaseca R and Corbalan R 1997 Second harmonic generation in a photonic crystal *Appl. Phys. Lett.* **70** 702–4
[42] Mills D 1991 *Nonlinear Optics* (Berlin: Springer)
[43] Mihalache D, Mazilu D, Crasovan L-C, Torner L, Malomed B and Lederer F 2000 Three-dimensional walking spatiotemporal solitons in quadratic media *Phys. Rev.* E **62** 7340–7
[44] Mou S, Lin C-F and Chou H-F 2001 Quasi-3-D beam-propagation method for modeling nonlinear wavelength conversion *J. Lightwave Technol.* **19** 772–9
[45] Nijhof J H B, Forysiak W and Doran N J 2000 The averaging method for finding exactly periodic dispersion-managed solitons *IEEE J. Sel. Top. Quantum. Electron.* **6** 330–6
[46] Schiff L 1968 *Quantum Mechanics* (New York: McGraw-Hill)
[47] Saleh B and Teich M 1991 *Fundamentals of Photonics* (New York: Wiley)
[48] Scalora M, Bloemer M J, Manka A S, Dowling J P, Bowden C M, Viswanathan R and Haus J W 1997 Pulsed second-harmonic generation in nonlinear, one-dimensional, periodic structures *Phys. Rev.* A **56** 3166–74
[49] Simonneau C, Debray J P, Harmand J C, Vidakovic P, Lovering D J and Levenson J A 1997 Second-harmonic generation in a doubly resonant semiconductor microcavity *Opt. Lett.* **22** 1775–7
[50] Steel M J and de Sterke C M 1996 Parametric amplification of short pulses in optical fiber Bragg gratings *Phys. Rev.* E **54** 4271–84
[51] Stein E 1993 *Harmonic Analysis. Real-Variable Methods, Orthogonality, and Oscillatory Integrals* (Princeton, NJ: Princeton University Press)
[52] de Sterke C M, Salinas D G and Sipe J E 1996 Coupled-mode theory for light propagation through deep nonlinear gratings *Phys. Rev.* E **54** 1969–89
[53] de Sterke C M, Eggleton B J and Krug P A 1997 High-intensity pulse propagation in uniform gratings and grating superstructures *J. Lightwave Technol.* **15** 1494–502
[54] Reed M and Simon B 1978 *Analysis of Operators* vol 4 (New York: Academic)
[55] Tarasishin A, Zheltikov A and Magnitskii S 1999 Matched second-harmonic generation of ultrasoft laser pulses in photonic crystals *JETP Lett.* **70** 819–25
[56] Teytel M 1999 How rare are multiple eigenvalues? *Commun. Pure Appl. Math.* **52** 917–34
[57] Di Trapani P, Caironi D, Valiulis G, Dubietis A, Danielius R and Piskarskas A 1998 Observation of temporal solitons in second-harmonic generation with tilted pulses *Phys. Rev. Lett.* **81** 570–3
[58] Trull J, Vilaseca R, Martorell J and Corbalan R 1995 Second-harmonic generation in local modes of a truncated periodic structure *Opt. Lett.* **20** 1746–8
[59] Uhlenbeck K 1976 Generic properties of eigenfunctions *Am. J. Math.* **98** 1059–78
[60] Weiner A M, Kan'an A M and Leaird D E 1998 High-efficiency blue generation by frequency doubling of femtosecond pulses in a thick nonlinear crystal *Opt. Lett.* **23** 1441–3
[61] Whitham G 1974 *Linear and Nonlinear Waves* (New York: Wiley)
[62] Yariv A and Yeh P 1984 *Optical Waves in Crystals* (New York: Wiley)
[63] Yasui T and Koshiba M 2001 Three-dimensional vector beam-propagation method for second harmonic generation analysis *J. Lightwave Technol.* **19** 780–5
[64] Hheng Z and Weiner A M 2001 Coherent control of second harmonic generation using spectrally phase coded femtosecond waveforms *Chem. Phys.* **267** 161–71
[65] Zhu Y and Ming N 1999 Dielectric superlattices for nonlinear optical effects *Opt. Quantum. Electron.* **31** 1093–128